

Regulation of *KCNQ1* and *CFTR* in Colorectal Cancer

A Thesis SUBMITTED TO THE FACULTY OF
UNIVERSITY OF MINNESOTA
BY

Rebecca A. Madden

IN PARTIAL FULFILLMENT OF THE REQUIREMENTS
FOR THE DEGREE OF
MASTER OF SCIENCE

Dr. Patricia Scott, Dr. Robert Cormier

May 2019

Acknowledgements

I would like to thank my friends and my family. You have helped me so much throughout my life, words cannot begin to explain what you mean to me. I will only say thank you and know that you know how much you have changed my life. I could never have reached where I am without your constant love and support. Also, I would like to thank my advisors, Dr. Patricia Scott and Dr. Robert Cormier and the other two members of my thesis committee, Dr. Glenn Simmons and Dr. Matthew Slattery who have given me so much research and career advice over the years. I'd also like to thank Dr. Cara Hegg, Dr. Sarah Lacher, Lysie Radovich, and Dr. Dan Levings who helped me with many of my research techniques and data analysis. And I'd like to give a special thank you to my lab members Kyle Anderson and Mekhla Singhania, and office mate Jennifer Krzarnich. You all helped me become a better researcher and were always there for me: I couldn't have done it without you!

I would also like to thank my funding sources: Integrated Biosciences Program for allowing me to be a graduate teaching assistant every semester, and for three years of summer funding. I would also like to acknowledge the lab funding sources: Whiteside Research Institute, the Randy Shaver Cancer Research Fund, and Essentia Health. I am extremely grateful for this funding which allowed me to undertake this great opportunity.

And finally, I'd like to thank our collaborators at the University of Minnesota Twin Cities, David Largaespada, Tim Starr, Gerry O'Sullivan, Ying Zhang, and Alex Khoruts and our collaborators at the Netherlands Cancer Institute, Amsterdam- Remond Fijneman, Gerrit Meijer, Jeroen Goos, and Sjoerd den Uil.

Abstract

Colorectal cancer is the 2nd deadliest cancer in the US with more than 50,000 deaths in 2017. Our group has identified *KCNQ1* and *CFTR* as colorectal cancer tumor suppressors. *KCNQ1*-low as well as *CFTR*-low expressing tumors have significantly poorer prognosis than high expressers: *KCNQ1*-low in stages II, III and IV colorectal cancer; *CFTR*-low in stage II. Thus, it is important to understand how *KCNQ1* and *CFTR* are downregulated in these poor prognosis cancers. *KCNQ1* and *CFTR* are expressed at the base of the intestinal crypt, the site of the stem cell compartment and origin of colorectal cancer. The Wnt/ β -catenin signaling pathway is important in determining stemness and is dysregulated in >85% of human colon cancers. Therefore, I am testing two hypotheses involving Wnt/ β -catenin and these tumors suppressors: 1) *KCNQ1* is regulated through a putative enhancer region containing a β -catenin binding site and 2) *KCNQ1* and *CFTR* regulate β -catenin activity.

Our putative enhancer region was identified through a survey of the *KCNQ1* genomic sequence for eQTLs (SNPs associated with altered expression of *KCNQ1*) which identified SNP rs2283155 in *KCNQ1* intron 2. SNPs are markers for potential polymorphic variants associated with altered gene expression. The enhancer region includes the SNP rs2283155, a TCF7L2 binding site (the binding partner of transcriptionally active β -catenin) and a larger DNase I hypersensitivity enhancer region. Luciferase reporter assays showed regulation by our enhancer region of a reporter gene. Follow-up data has suggested that *KCNQ1* is the gene being regulated.

Second, to investigate the effect of *Kcnq1* and *Cftr* on β -catenin signaling, I am examining β -catenin in organoids, a well-established model of the stem cell compartment.

Activation of β -catenin is characterized by its movement from the cytoplasm or membrane to the nucleus. I developed an immunofluorescence assay to quantitatively measure nuclear β -catenin localization in *Kcnq1* deficient/expressing and *Cftr* deficient/expressing organoids. These organoids had increased β -catenin activity in *Kcnq1*-deficient and *Cftr*-deficient organoids, suggesting a mechanism for tumor suppressor activity of *Kcnq1* and *Cftr*. This work may provide insight into the role of *Kcnq1* and *Cftr* within the cellular environment and potential ways to manipulate their expression to improve survival.

Table of Contents

Acknowledgements.....	i
Abstract.....	ii
Table of Contents.....	iii
List of Figures.....	iv
Introduction.....	1
Chapter 1: Regulation of <i>KCNQ1</i> by β -catenin and <i>KCNQ1OT1</i>	
Materials and Methods.....	26
Results.....	31
Discussion.....	48
Chapter 2: Regulation of β -catenin by <i>CFTR</i> and <i>KCNQ1</i>	
Materials and Methods.....	53
Results.....	58
Discussion.....	69
Appendix	73
Additional	78
References.....	79

List of Figures

Figure 1. Colorectal Cancer statistics	1
Figure 2. Structure of small intestine and colon epithelial tissue.....	3
Figure 3. Intestinal stem cell compartment	4
Figure 4. Wnt/ β -catenin pathway	6
Figure 5. Colorectal Cancer survival	10
Figure 6. Vogelgram	11
Figure 7. Colorectal Cancer patient survival stratified by <i>KCNQ1</i> expression	14
Figure 8. <i>KCNQ1</i> role in cell	15
Figure 9. <i>KCNQ1OT1</i> imprinting pattern	17
Figure 10. <i>KCNQ1</i> interactions	20
Figure 11. Luciferase reporter assay	30
Figure 12. Expression of <i>KCNQ1</i> and <i>KCNQ1OT1</i>	31
Figure 13. siRNA Knockdown of <i>KCNQ1OT1</i>	32
Figure 14. siRNA Knockdown of β -catenin	33
Figure 15. <i>KCNQ1</i> expression stratified by SNP rs2283155	34
Figure 16. Putative enhancer region	35
Figure 17. Reporter plasmid pLS-LR	36
Figure 18. Luciferase reporter assay: <i>LDHA</i> plasmid	37
Figure 19. Luciferase reporter assay: <i>LDHA</i> and <i>NQO1</i> plasmid	37
Figure 20. Luciferase reporter assay: TCF7L2 and TDHS_C constructs plasmid	38
Figure 21. Luciferase reporter assay: Wnt experiment	39
Figure 22. Luciferase reporter assay: Freezing experiment	40
Figure 23. Luciferase reporter assay: Hct116 compared to HEK293	40
Figure 24. Luciferase reporter assay: Final results	42
Figure 25. RT-qPCR results	43
Figure 26. 4C data collection	44
Figure 27. Virtual 4C raw data readout	46
Figure 28. Virtual 4C normalized data readout	46
Figure 29. Immunofluorescent staining of organoids	56
Figure 30. Organoid IFC: First attempts	60
Figure 31. Organoid IFC: fixed 24 hours after plating	60
Figure 32. Organoid IFC: DAPI experiment	61
Figure 33. Organoid IFC: First β -catenin	62
Figure 34. Organoid IFC: β -catenin with saponin.....	62
Figure 35. Organoid IFC: Control: Wnt/GSK3 inhibitor treatment	63
Figure 36. Verification of <i>Apc</i> loss in organoids	64
Figure 37. Organoid IFC: Control: <i>Apc</i> high and low organoids	65
Figure 38. Organoid IFC: <i>Cftr</i> KO/WT	67
Figure 39. Organoid IFC: <i>Kcnq1</i> KO/WT	68
Figure 40. <i>Cftr</i> interactions	70
Figure 41. <i>Kcnq1</i> interactions	71
Figure 42. Unfolded protein response	73
Figure 43. MTT Assay with Y21 and D8	76
Figure 44: SRB Assay with Y21 and D8	77

Introduction

Colorectal Cancer

Across the globe, colorectal cancer is the second most common cancer, with more than 1.8 million cases reported in 2018 alone (World Cancer Research Fund). In the United States, colorectal cancer is estimated to affect more than 140,000 people and will kill more than 50,000 this year (NIH 2018). 8.1% of all new cancer cases and 8.3% of cancer deaths are due to colorectal cancer (NIH 2018). This is a very significant percentage when one considers the many different types of cancers that exist. From 1992 to 2015, both the incidence and mortality of colorectal cancer have decreased, however, the number of people affected still remains troublingly high (Figure 1).

There are several possible reasons for the high mortality rate. Many cases of colorectal cancer are not detected until later stages, and prognosis for these patients is significantly worse (Siegel *et al.*, 2017). Another problem is that certain cases of colorectal cancer have worse prognosis compared to other cases at the same clinical stage (Taieb *et al.*, 2017). Many biomarkers have been identified to help predict colorectal

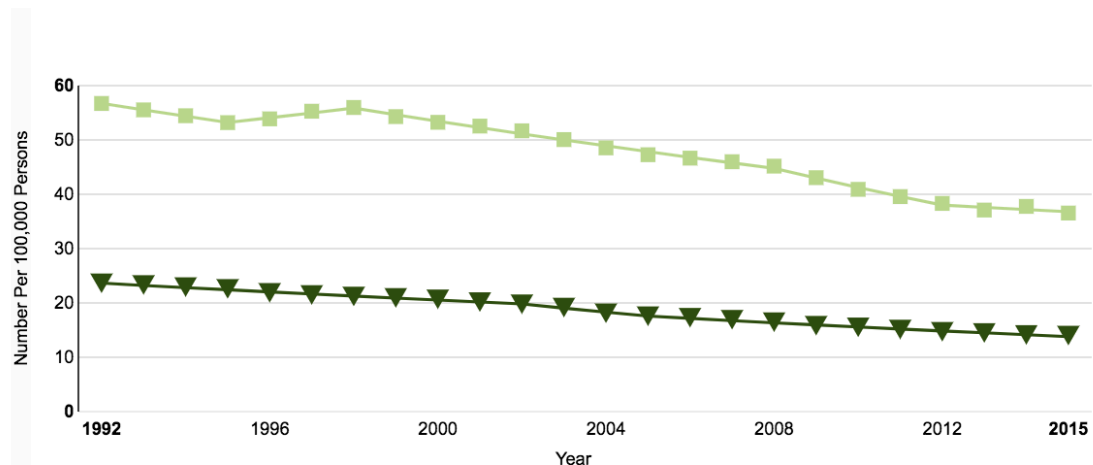


Figure 1: Incidence and mortality rates of colorectal cancers from 1992 to 2015. New cases are in light green, deaths are in dark green. NIH, 2015.

cancer prognosis (Bramsen *et al.*, 2017). Biomarkers are genes whose expression is associated with cancer. More biomarkers are necessary to determine cancer aggressiveness and to assist with earlier detection of colorectal cancer. Most importantly, some biomarkers play a causal role as well as a diagnostic role, and the identification of such genes is beneficial for the development of therapeutic targets.

Colorectal cancers are either sporadic or hereditary. Within these broader categories, there are two types, MSS (microsatellite stable) or MSI (microsatellite instable). Microsatellites are long, sequence repeats with high mutation rates when the DNA mismatch repair mechanism is not functional (Fleming, Ravula, Tatishchev, & Wang, 2012). MSI colorectal cancers' microsatellite regions vary in length, while MSS colorectal cancers microsatellite regions do not (Fleming *et al.*, 2012). MSI colorectal cancers make up about 15% of all sporadic colorectal cancers, and nearly all hereditary colorectal cancers (Xiao & Freeman, 2015). MSI type patients have longer disease-free survival as well as overall survival (Hong *et al.*, 2012). Moreover, the MSI type of colorectal cancer is the only type that responds significantly to immunotherapy treatments (Kather, Halama, & Jaeger, 2018). Immunotherapy is a process of modifying the immune system to recognize and fight cancer cells which has proved very promising in many different types of cancer (Duong, 2014). However, MSS colorectal cancer, making up the other 85% of all sporadic colorectal cancers, is the more aggressive form of colorectal cancer, and remains unresponsive to most immunotherapies.

Intestinal Structure and Signaling pathways

Colorectal cancer develops in the epithelial layer of the gastrointestinal tract. The epithelial layer of the intestine is comprised of a single layer of cells. In the small intestine, there are structures called villi which protrude toward the center of the intestine (Figure 2). Villi are formed by cellular proliferation within the crypt, causing outward migration of those cells. These villi greatly increase the surface area of the small intestine increasing absorption of nutrients. There are also invaginations of the epithelial tissue that enfold away from the lumen of the intestine, forming small crypt structures. The colon has crypts; however, they do not have villi.

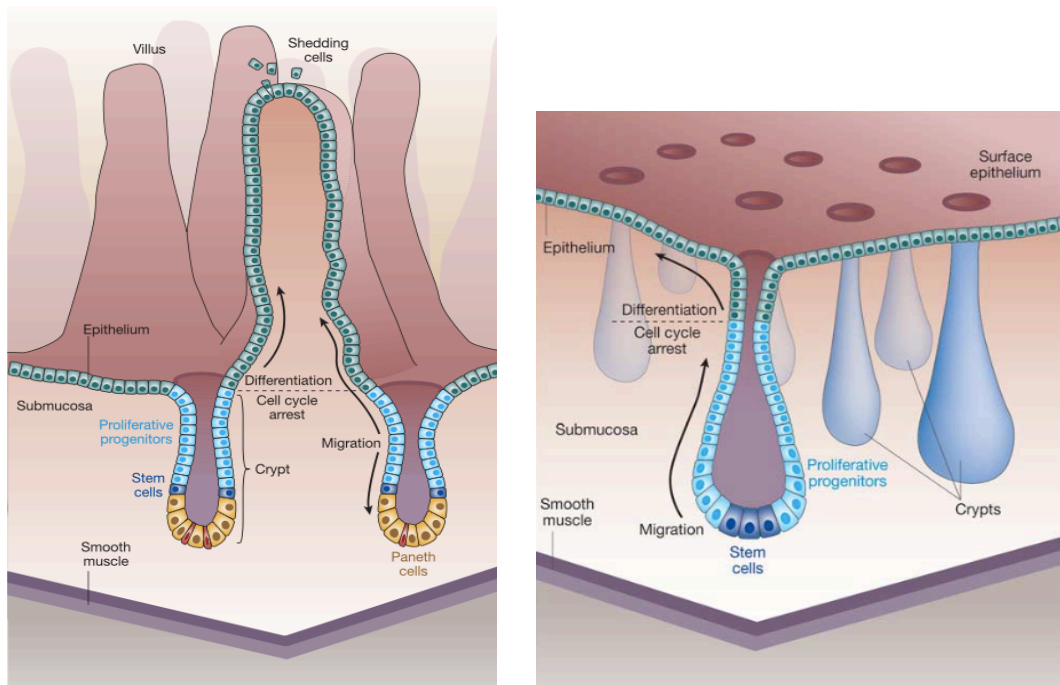


Figure 2: Structure of small intestinal (left) and colon epithelial tissue (right). Both have crypt structures, where the stem cells are located. However, the small intestine has villi structures which extend into the intestinal lumen, while the colon does not. Reya and Clevers, 2005.

These crypts provide protection to the stem cells located at the base. Stem cells are vital for the regeneration of the epithelial tissue through the process of stem cell

differentiation. This process occurs approximately every seven days (Reya & Clevers, 2005), beginning with stem cells at the base of the crypt, usually about six stem cells in total (Reya & Clevers, 2005). Following asymmetric cell division, stem cells produce daughter cells that differentiate into a set of cells referred to as the proliferative progenitors, enterocyte progenitors, or transit amplifying cells (Tettah *et al.*, 2016; Flier & Clever, 2009; Haegerbarth & Clevers, 2009). From this intermediate form, the cells differentiate into their final form: either goblet cells, enteroendocrine cells, secretory enterocytes, or absorptive enterocytes (Flier & Clevers, 2009). As the cells differentiate, they move upward until they reach the top of the crypts, where they are sloughed off into the epithelial lumen. There is a rapid turnover of epithelial tissue, as the intestinal environment is very harsh. Until recently, it was thought that this stem cell differentiation pathway could only progress in the one direction, however, recent studies have found that dedifferentiation of intestinal cells back into stem cells can occur (Schwitalla *et al.*, 2013; *et al.*, 2016).

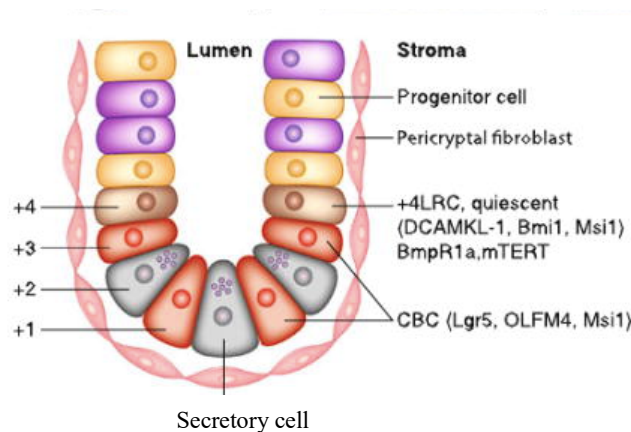


Figure 3: Intestinal stem cell compartment and differentiated epithelial cells Anderson *et al.*, 2011.

Intestinal stem cells are known to express the *LGR5* gene, a Wnt target gene encoding a transmembrane protein (Zeuner *et al.*,2014; Haegerbarth & Clevers, 2009). These stem cells have “stemness”, or an ability to self-renew and differentiate into a varied subset of cells (Zeuner *et al.*,2014). There are two subpopulations of stem cells: crypt base cells and +4 cells. The crypt base cells are marked by the LGR5 stem cell marker, and are in an active state (Barker *et al.*, 2007). These crypt base cells also commonly express Ki67, a cellular marker for proliferation (Barker *et al.*,2007). The LGR5+ stem cells are rapidly dividing, but they divide much more slowly in the colon than in the small intestine (Barker *et al.*,2007).

The other subpopulation of stem cells that do not express the *LGR5* gene are classified as the 4+ LRC stem cells (Barker *et al.*,2007; (Umar, 2010). These cells are so named because they are found at position 4 in the intestinal crypt. These 4+ cell express specific stem cell markers, including DCAMKL-1, Bmi1, Msi1, BmpR1a, mTERT (Umar, 2010). While the LGR5+ cells are constantly dividing, the 4+ cells do not undergo rapid cell division. They are normally quiescent, or in a dormant state (Umar, 2010). These +4 stem cells are suspected to be a reservoir for renewing both the intestinal epithelial cells and the intestinal stem cells (Kabiri 2018; Beumer & Clevers, 2016).

The characteristics of stem cells are controlled by many signaling pathways, the most important being the Wnt/ β -catenin pathway. The canonical Wnt/ β -catenin regulatory pathway (Figure 4) is one of the most influential pathways in the intestinal crypt, affecting the dynamics of the crypt, the stem cells, and influencing the development of colorectal cancer (Clevers, 2006). There are also two noncanonical Wnt

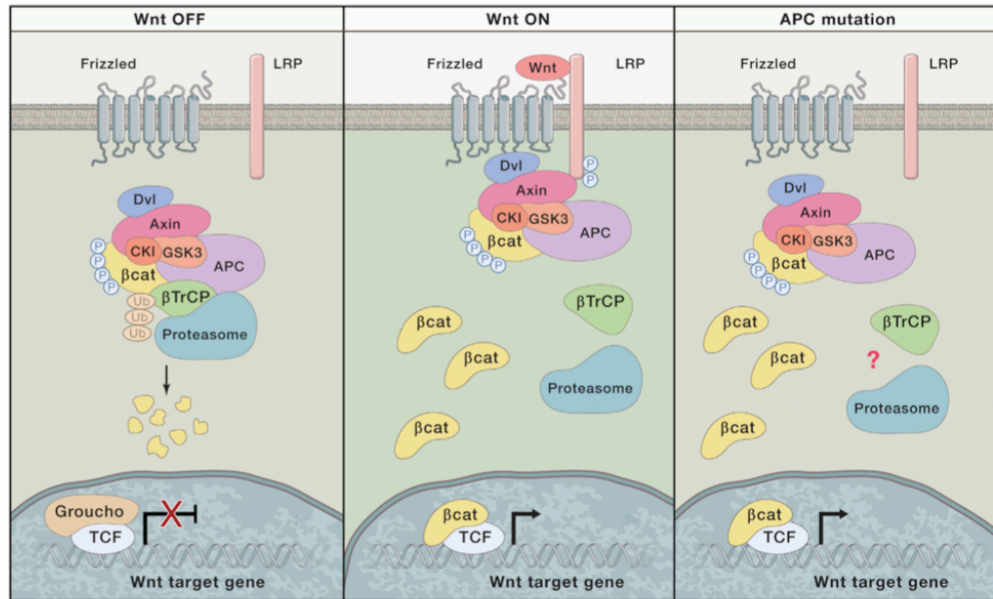


Figure 4: Canonical Wnt/ β-catenin pathway. Nusse & Clevers, 2017.

receptor pathways: the Wnt/PCP pathway and the Wnt/Ca²⁺ pathway (Zhan, Rindtorff, & Boutros, 2017).

In colorectal cancer, the canonical Wnt/ β-catenin is known to play a significant role (Clevers, 2006; Zhan, Rindtorff, & Boutros, 2017). Wnt is a regulatory ligand protein, released by secretory cells within the intestinal crypt. It binds to the transmembrane protein Frizzled, which is complexed with LPR (low-density lipoprotein receptor-related protein) and several other proteins (Nusse & Clevers, 2017). The binding of Wnt triggers the release of β-catenin from the destruction complex, a major factor of which is the APC (adenomatous polyposis coli) protein (Zhan, Rindtorff, & Boutros, 2017). This leaves the β-catenin protein in the cytoplasm available for translocation into the nucleus. Inside the nucleus, the β-catenin acts as a transcription factor, binding to a TCF factor, causing its derepression and inducing expression of proliferation genes (Zhan, Rindtorff, & Boutros, 2017). β-catenin also induces the expression of genes which maintain stemness of the stem cell (He *et al.*, 2004). Another

important gene induced by the Wnt/ β -catenin pathway is *LGR5*. *LGR5* is a receptor for R-spondin, a secreted protein that induces the Wnt/ β -catenin pathway (de Lau *et al.*, 2011).

This pathway regulates the intestinal stem cells through a precise gradient of Wnt throughout the crypt (Reya 2005). The highest Wnt/ β -catenin activity is observed at the base of the crypt, indicated by the high expression Wnt target proteins (Flier & Clevers, 2009). The Wnt/ β -catenin pathway determines whether the epithelial cells of the crypt are going to proliferate or differentiate (Flier & Clevers, 2009). High Wnt/ β -catenin signaling induces higher proliferation, while lower induces differentiation (Flier & Clevers, 2009). If Wnt is not present in the cellular environment, cell proliferation is halted, and the crypt epithelium will die off (Mah, Yan, & Kuo, 2016). If Wnt is overexpressed throughout the crypt, over proliferation occurs (Flier & Clevers, 2009). The cells most exposed to Wnt/ β -catenin are the stem cells. These are the only cells to have significant β -catenin staining in the crypt in a non-cancer situation (Flier & Clevers, 2009). In colorectal cancer, the canonical Wnt/ β -catenin pathway is known to play a significant role (Clevers, 2006; Zhan, Rindtorff, & Boutros, 2017). If the regulation of Wnt/ β -catenin is lost, it has very serious consequences. The Wnt/ β -catenin pathway is dysregulated in 85% of all sporadic colorectal cancers.

Another important pathway in stem cell maintenance is the Notch pathway, which also plays a major role in the fate of cells after differentiation from the stem cell state (Flier & Clevers, 2009). The Notch pathway helps to balance the proliferation and differentiation of cells within the intestine (Sancho, Cremona, & Behrens, 2015). The Notch pathway involves interaction between two membrane spanning proteins on

adjacent cells, a receptor, known as Notch, and a ligand, known as Delta or Jagged. The Notch receptor first binds to a Notch ligand, which results in cleaving of the receptor (Sancho, Cremona, & Behrens, 2015). This leaves the intracellular portion of the Notch receptor (NICD) available in the cytoplasm to localize to the nucleus (Flier & Clevers, 2009). Once in the nucleus it binds to the transcription factor RBP-J to activate Notch target genes (Sancho, Cremona, & Behrens, 2015). The target genes include *HES1*, which prevents expression of *MATH1*. *MATH1* expression is necessary for the differentiation of the secretory cells (Flier & Clevers, 2009). When *HES1* is expressed instead of *MATH1*, the cells differentiate into absorptive enterocytes (Flier & Clevers, 2009).

The TGF- β pathway also plays an important role in homeostasis in the intestinal crypt environment, through its regulation of fibrosis and immune response modulation. The TGF- β is expressed in a gradient throughout the crypt, with higher expression towards the top of the crypt and lower expression toward the bottom (Cammareri *et al.*, 2017). This is the opposite of the Wnt/ β -catenin pathway. TGF- β proteins act through the SMAD pathway. TGF- β first binds to the complexed receptors BMPR1 and BMPR2 (Cammareri *et al.*, 2017). BMPR2 phosphorylates the BMPR1 receptor, which then phosphorylates the bound SMADs (R-Smad) factor (Katz *et al.*, 2016). SMADs then binds to SMAD4, and this complex moves into the nucleus, where it can act as either an activator or a repressor of specific target genes (Spit *et al.*, 2018). Some of the target genes include *E-cadherin*, collagen, and integrins; this SMAD complex has also been observed to interact with *RUNX*, a tumor suppressor gene (Katz *et al.*, 2016).

Together, these pathways play a vital role in the maintenance and regulation of the stem cell compartment. These intestinal stem cells in turn maintain the crypt, providing new cells that are continually lost to the harsh intestinal environment. Intestinal stem cells are essential to regenerate the healthy intestinal epithelium, but because of this capacity when dysregulated they can become cancer stem cells.

Cancer Stem Cells in Colorectal Cancer

Cancers are extremely heterogeneous, containing many different types of cells, and continually evolve in response to changes in their environment (Kreso & Dick, 2014). Many models have been developed to try to explain how cancers evolve. The somatic evolution model suggests that a mutant tumor cell has a growth advantage and outcompetes the other surrounding cells (Greaves & Maley, 2012). However, that model doesn't full explain some dynamics of tumor development, such as the presence of a small population of cells with variable proliferation and tumorigenesis properties (Chen, Dong, Haiech, Kilhoffer, & Zeniou, 2016). These subpopulations of cells are called cancer stem cells.

Cancer stem cells may have plasticity, the ability to transition from highly oncogenic states to lesser oncogenic states and back again (Cabrera, Hollingsworth, & Hurt, 2015). This plasticity allows for even greater adaptability within tumors (Cabrera, Hollingsworth, & Hurt, 2015). Intestinal stem cells and progenitor cells are able to transition to into cancer stem cells. This produces a highly dynamic intestinal tumor which can adapt rapidly to its environment (Zeuner *et al.*, 2014).

The presence of cancer stem cells has significant consequences for cancer treatments. Cancer stem cell quiescence can lead to resistance to cancer therapies, many of which target the highly proliferative cancer cells of a tumor (Zeuner *et al.*, 2014; Chen *et al.*, 2016). This resistance to therapy causes many cancer reoccurrences (Takeda *et al.*, 2018). The plasticity of these cancer cells provides yet another avenue of treatment resistance. If the cancer stem cells do happen to be removed by a cancer treatment, other cells can transition into cancer stem cells, making it very difficult to completely remove the cancer.

Development of Colorectal Cancer

Colorectal cancer advances through several stages of development. These stages are defined by several factors: size of tumor, depth of invasion through the various tissue layers of the intestine, and whether the tumor has spread from its original location (Figure 5; ACS, 2018). Stage 0 is the earliest stage of the cancer, whereupon the cancer has not

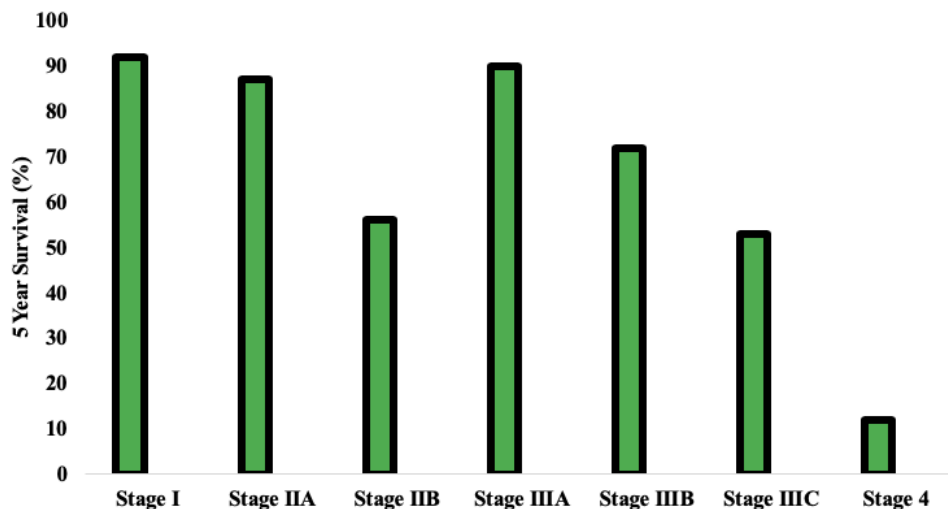


Figure 5: Survival percentage after five years for each stage of colorectal cancer. Prognosis remains relatively high in the early stages but decreases in more advanced stage II and III decreases drastically in stage IV. ACS 2018.

extended deeper than the inner layer, or the mucosa of the colon (Figure 5; ACS, 2018). Stage I colorectal cancer has invaded through the mucosal layer, but not farther (Figure 5; ACS, 2018). Stage II colorectal cancer has grown into all layers of colon (Figure 5; ACS, 2018). Stage III colorectal cancers have grown into all layers of colon as well as invaded several nearby lymph nodes (Figure 5: ACS 2018). Stage IV colorectal cancers have metastasized from the original tumor to distant organs or the peritoneum (Figure 5; ACS, 2018). Mortality is the highest in the later stages of colorectal cancer (Siegel *et al.*, 2017). Approximately 20% of colorectal cancer patients have metastasized cancer upon diagnosis (Riihimäki *et al.*, 2016). Survival of most colorectal cancer patients with metastases is only 30 months after diagnosis (Fakih, 2015).

Accumulation of Mutations in Colorectal Cancer

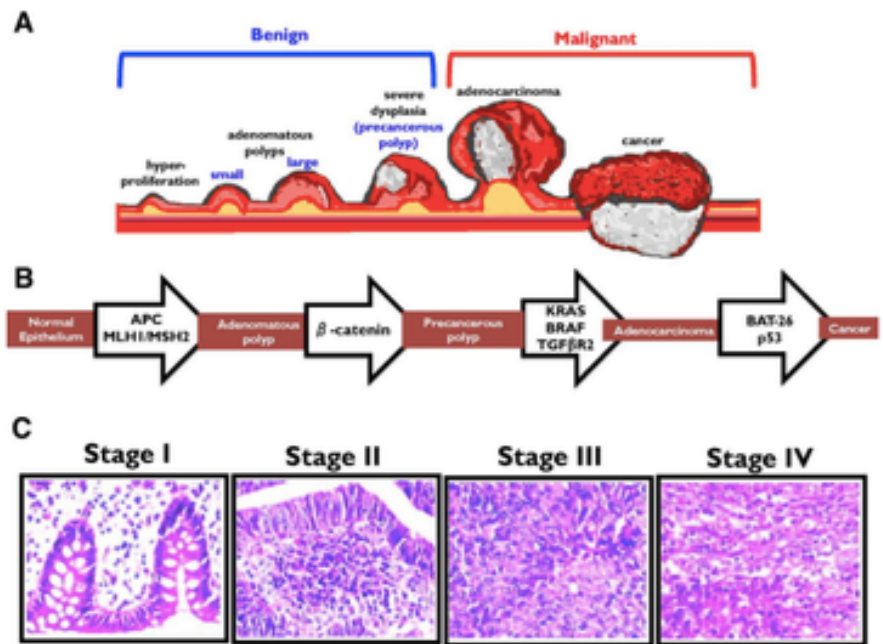


Figure 6: Vogelgram, demonstrates major mutations which drive progression of colorectal cancer (Senevitatne 2014).

As colorectal cancer develops, mutations accumulate in the tumors, leading to progression of the disease (Figure 6). The Vogelstein lab identified the most common mutations and associated them with different stages of colorectal cancer (Vogelstein and Fearon, 1990). One of the most commonly mutated genes was *APC*. Mutations in *APC* occur in 85% of sporadic colorectal cancers (Valkenburg, Graveel, Zylstra-Diegel, Zhong, & Williams, 2011) Inactivation of *APC* promotes the development of adenomas and maintains tumor development (Dow *et al.*, 2015). Mutations in *KRAS* (a gene responsible for cell proliferation regulation also) were found in about 40% of tumors. Mutations in *KRAS* promote the development of an early adenoma to a larger late stage adenoma. Other mutations, including *p53* and *BRAF* commonly occur, pushing the adenoma to an invasive carcinoma (Senevitatne 2014; (Rao & Yamada, 2013).

However, these mutations do not explain every aspect of colorectal cancer development. Vogelstein sequenced the exons of human colorectal cancer tumors, and found many mutations in each tumor (Fearon & Vogelstein, 1990). The challenge then becomes determining which of these mutations have a functional role in colorectal cancers.

Identification of Tumor Suppressor Gene KCNQ1

Forward genetic screens have been used to identify genes that are functionally important for development of colorectal cancer. A Sleeping Beauty (SB) transposon mutagenesis screen is a common tool for determining which mutations occur commonly in tumors (Starr *et al.*, 2009). A transposon is a segment of DNA that possesses the ability to move and replicate itself within the chromosome (Izsvák & Ivics, 2004).

Transposons are used as a tool for germ-line mutagenesis, the creation of mutations throughout the DNA (Izsvák & Ivics, 2004) . The phenotype of mutated organisms is then evaluated. This allows researchers to determine which genes are responsible for a particular biological function (Nolan, Kapfhamer, & Bućan, 1997) .

To determine which genes may be playing a significant role in the development of colorectal cancer, a Sleeping Beauty transposon mutagenesis screen was done to generate mutations in a wild-type background (Starr *et al.*, 2009). Transgenic mice were generated that carried a Sleeping Beauty transposon, a conditionally activated Sleeping Beauty transposase and a recombinase (Villin-Cre) to activate the transposase in the intestinal epithelium. Unlike wild-type mice, mice carrying these alterations developed intestinal tumors. The mice were sacrificed, dissected, and tumor tissues were collected. Their tumor DNA was sequenced to determine the genomic locations into which transposons had inserted. This resulted in an average of 124 insertions site mutations in each tumor (Starr *et al.*, 2009). The sites of these insertions were analyzed to determine which genes had more insertions than expected by chance. Genes that had more insertions than expected by chance are called common insertion sites. Since these genes had more insertions than expected by chance, the insertion must likely provide a selective advantage to the tumor. Therefore, these genes are considered candidate cancer-causing genes. 77 candidate cancer-causing genes were identified. At the top of this list was *Apc*, and also in the top 10 was a new candidate gene, *Kcnql1*. Examination of the literature revealed that the best understood role of *KCNQ1* in the intestine was to provide the electrical driving force for export of chloride ions by *CFTR*. *Cftr* was also a CIS gene in the list of 77 identified as candidate cancer-causing genes

To further explore the role of *Kcnq1* in colorectal cancer, *Kcnq1* was knocked out via a targeted deletion mutation in *Apc*^{Min} mice (Than *et al.*, 2014). The *Apc*^{Min} *Kcnq1* KO mice developed a 2-fold increase in gastrointestinal tumors compared to the *Apc*^{Min} *Kcnq1* WT mice, suggesting that *Kcnq1* has a role as a tumor suppressor (Than *et al.*, 2014). The *Kcnq1* KO mice also showed changes in their intestinal global gene expression, suggesting that the *Kcnq1* pathway plays a major role in the intestine (Than *et al.*, 2014). The changes in gene expression in the *Kcnq1*-deficient intestine were examined and was found to overlap with changes in gene expression in *Muc2*-deficient and *Cftr*-deficient intestine. This result suggests that *Muc2* and *Cftr* could be involved in the same pathway as *Kcnq1*, perhaps in a similar tumor suppressive role.

To examine the effect of *Kcnq1* on the stem cell compartment, organoids were developed from the intestinal crypts of the *Kcnq1* KO and WT mice. The *Kcnq1* KO organoids demonstrated a much higher clonogenicity, or ability to produce more

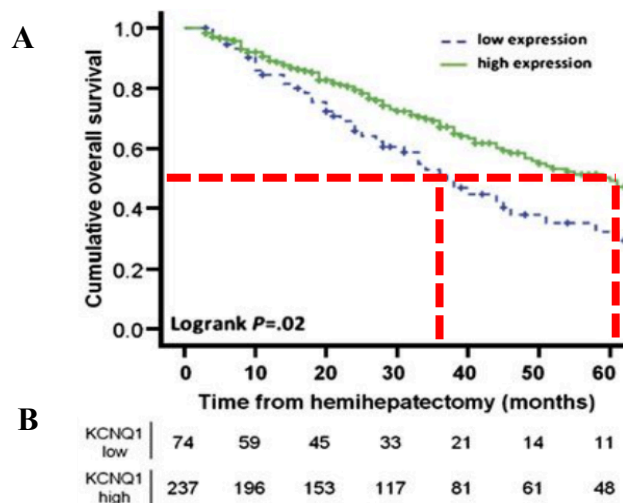


Figure 7: A) Cumulative overall survival for stage IV colorectal cancer patients with either high (green) or low (blue) expression of *KCNQ1*. High expression of *KCNQ1* results in extended survival by 23 months. B) The number of patients surviving at each time point, for both *KCNQ1* low and high expression. Than *et al.*, 2014.

organoids. As clonogenicity may be determined by the stem cells “stemness”, this suggests a regulatory role of *Kcnq1* within the intestinal stem cell (Than *et al.*, 2014).

To determine whether the observation of *Kcnq1* deficiency driving tumorigenesis in mice was true in humans, *KCNQ1* expression was studied within human tumor samples collected from 500 stage IV colorectal cancer patients with liver metastases (Than *et al.*, 2014). These patients all had hemihepatectomy, the removal of one or more lobes of the liver (Than *et al.*, 2014). Of the 500 patients, *KCNQ1* expression was examined in 311 of those patients, and it was found that higher expression of *KCNQ1* correlated with better median survival for these patients by a highly significant 23 months (Figure 7; Than *et al.*, 2014). Therefore, it was concluded that *KCNQ1* is a tumor suppressor in human colorectal cancer.

KCNQ1

KCNQ1, potassium voltage-gated channel subfamily Q member 1, is located on chromosome 11p15.5, encoding a voltage-gated potassium channel. This channel allows

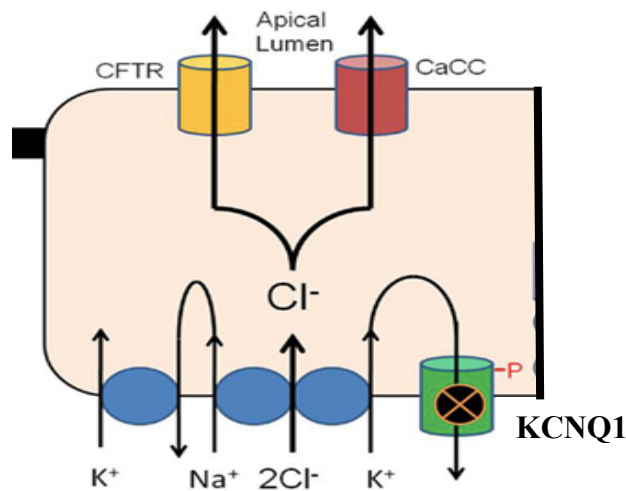


Figure 8: Role of *KCNQ1* in cell. *KCNQ1* channel, located on basolateral membrane, allows movement of intracellular potassium out of the cell. Alzamora *et al.*, 2011.

the movement of potassium out of the cell (Figure 8; Alzamora *et al.*, 2011). The channel is located on the plasma membrane of the cell, and is expressed in various locations throughout the body, including the heart, kidney, inner ear, and the gastrointestinal tract (Abbott, 2014). In the intestine, *KCNQ1* is expressed within the intestinal crypt, in the stem cell compartment (Alwan unpublished; Preston *et al.*, 2010; Jadhav *et al.*, 2017; Schroeder *et al.*, 2000). *KCNQ1* maintains water and ion homeostasis within the epithelial tissue cells (Warth *et al.*, 2002). In mice with *KCNQ1* KO, the cellular ionic balance was disrupted. A lack of functional potassium channels prevented the movement of potassium into the basolateral extracellular space. Due to this altered ionic gradient, chloride ions were prevented from moving into the apical extracellular space also (Warth *et al.*, 2002).

Alteration and mutations in *KCNQ1* are linked to many other disorders besides colorectal cancer. Mutations in *KCNQ1* have been seen in long QT syndrome, a condition of the heart wherein repolarization of the ventricular tissue is elongated. This condition can cause cardiac arrhythmias, which can cause death (Crotti *et al.*, 2008). Mutations in *KCNQ1* are also associated with Jervell and Lange-Nielson syndrome, a rare disorder that causes deafness as well as long QT syndrome (Than *et al.*, 2014; (Vyas *et al.*, 2016). Moreover, *KCNQ1* mutations have been indicated as a susceptibility gene for Type 2 diabetes (Kasuga, 2011). *KCNQ1* mutations also play a role in epilepsy development, often in conjuncture with long QT syndrome (Villa & Combi, 2016).

Although the regulation of *KCNQ1* is not completely understood, two factors are thought to play a role, *KCNQ1OT1* and β -catenin. *KCNQ1OT1* is a long non-coding RNA which is encoded within intron 10 of *KCNQ1*. β -catenin is a protein usually found

near the cell membrane and in the cytoplasm but when localized to the nucleus acts as a transcription factor to induce proliferation (Zhan *et al.*, 2017). Both these factors are thought to regulate *KCNQ1*, but their particular roles are very complicated.

KCNQ1OT1 is an imprinted gene that encodes an antiparallel long non-coding RNA which regulates *in cis* the other genes in its domain. An imprinted gene is monoallelically expressed due to a developmental epigenetic silencing of one allele. (Chiesa *et al.*, 2012). *KCNQ1OT1* contains a promoter CpG island that when methylated results in silencing of transcription. *KCNQ1OT1* is normally methylated on the maternal gene and expressed only on the paternal gene (Figure 9; Chiesa *et al.*, 2012). (Kanduri, 2016). Methylation is regulated and maintained through the activity of enzymes called DNA methyltransferases, or DNMTs (Scott *et al.*, 2014). This methylation patterning is extremely important to control gene expression levels in the various stages of development (Kanduri 2016).

When mutations and alterations occur that cause changes in the methylation pattern of *KCNQ1OT1*, many problems can occur. If *KCNQ1OT1* is hypomethylated,

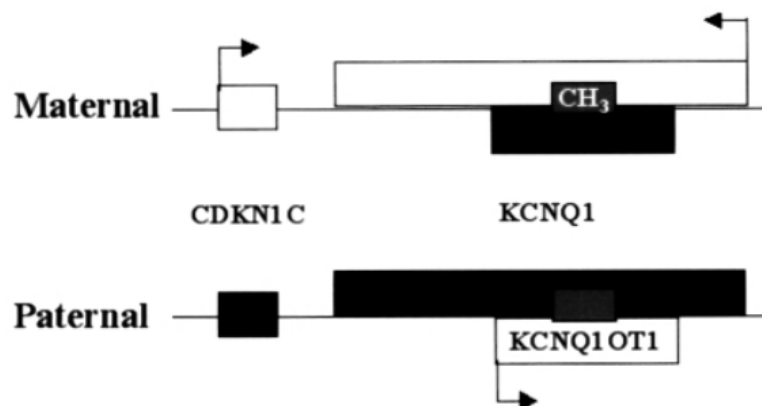


Figure 9: Imprinting paternal of *KCNQ1OT1*. *KCNQ1OT1* is methylated on the maternal alleles, and only expressed on the paternal allele (Weksberg 2002). White genes are expressed, black genes are not expressed

both alleles of *KCNQ1OT1* are expressed. This can lead to Beckwith-Wiedemann syndrome (Weksberg *et al.*, 2003). Beckwith-Wiedemann syndrome is a complicated disease which can result in infant overgrowth, failure of the abdominal wall to develop properly, and an increased risk for tumor development (H'mida Ben-Brahim *et al.*, 2015). Even if *KCNQ1OT1* is partially hypomethylated, it can lead to a mosaic of differential expression of *KCNQ1OT1* throughout tissues (H'mida Ben-Brahim *et al.*, 2015). Another common disease associated with aberrant methylation of *KCNQ1OT1* is Silver-Russell syndrome (Eggermann, Eggermann, & Schönherr, 2008). This syndrome results in growth retardation and *KCNQ1OT1* is often hypermethylated, resulting in decreased *KCNQ1OT1* expression (Eggermann, Eggermann, & Schönherr, 2008). Therefore, there is a very delicate balance of gene expression conferred by this imprinting by methylation. If disturbed, it can have very serious outcomes for the individuals involved.

KCNQ1OT1 acts as a regulator to the genes in its domain (Pandey *et al.*, 2008). The full length of *KCNQ1OT1* must be expressed for regulation of the genes within its domain or the imprinted control region (ICR) (Mancini-DiNardo, Steele, LeVorse, Ingram, & Tilghman, 2006). *KCNQ1OT1* interacts with the DNA as well as with the histone methyltransferases H3K9 and H3K27, resulting in regulatory chromatin rearrangements (Pandey *et al.*, 2008; Jones, Bogutz, & Lefebvre, 2011; Kanduri 2011). *KCNQ1OT1* also is thought to interact with Dnmt1, a DNA methyltransferase, to regulate the gene silencing (Mohammad, Mondal, Guseva, Pandey, & Kanduri, 2010). *KCNQ1* and other genes are expressed within the *KCNQ1OT1* domain (Korostowski *et al.*, 2012). *KCNQ1OT1* is thought to inhibit expression of the genes of this domain.

However, there has been mixed data whether or not *KCNQ1* is also regulated by *KCNQ1OT1* (Pandey *et al.*, 2008). *KCNQ1* has been reported to be regulated by *KCNQ1OT1* expression in blood leukocytes (Valente *et al.*, 2019). On the other hand, it has been reported in mouse heart tissue that although *KCNQ1OT1* down regulates the expression of other genes in the domain, the expression of *KCNQ1* is independent to the imprinting of *KCNQ1OT1* (Korostowski *et al.*, 2012). These data suggest that there is more regulation occurring within this gene domain than just the activity of *KCNQ1OT1*. One possibility is the presence of enhancers within the *KCNQ1OT1* ICR (Schultz *et al.*, 2015). These enhancers may counteract the activity of downregulation by *KCNQ1OT1*, allowing expression of the genes within this imprinted region (Schultz *et al.*, 2015).

The other major candidate for regulation of *KCNQ1* is the transcription factor β -catenin. β -catenin is the major component of the Wnt/ β -catenin pathway which plays such a pivotal role in colorectal cancer. We would expect to see a negative correlation between *KCNQ1* and β -catenin, as β -catenin is a pro-cancer transcription factor, and *KCNQ1* is a tumor suppressor. However, there are contradicting results in the literature. In colorectal cancer cell lines, *KCNQ1* and β -catenin interact bidirectionally. When *KCNQ1* expression is decreased, β -catenin moves from the membrane into the cytoplasm, when *KCNQ1* is increased, β -catenin moves from the cytoplasm back into the membrane, and β -catenin in the nucleus leads to decreased *KCNQ1* expression (Rapetti-Mauss *et al.*, 2017).

There are several papers that suggest a positive correlation between *KCNQ1* and β -catenin expression. In oocytes, increased β -catenin expression in the plasma membrane has been correlated with increased *KCNQ1* expression in the cytoplasm and plasma

membrane (Wilmes *et al.*, 2012). In human colorectal cancer protein data, nuclear β -catenin was correlated to increased *KCNQ1* protein expression (den Uil *et al.*, 2016). β -catenin in the nucleus has also been shown to increase the expression of *KCNQ1* via increased activity of *SGK1*-a serine/threonine protein kinase (Strutz-Seebohm *et al.*, 2009). Therefore, there is much conflicting evidence as to the relationship between *KCNQ1* and β -catenin (Figure 10). There is yet another layer of complexity in the interactions between β -catenin and *KCNQ1*, as β -catenin itself is thought to regulate *KCNQ1OT1* expression (Sunamura *et al.*, 2016).

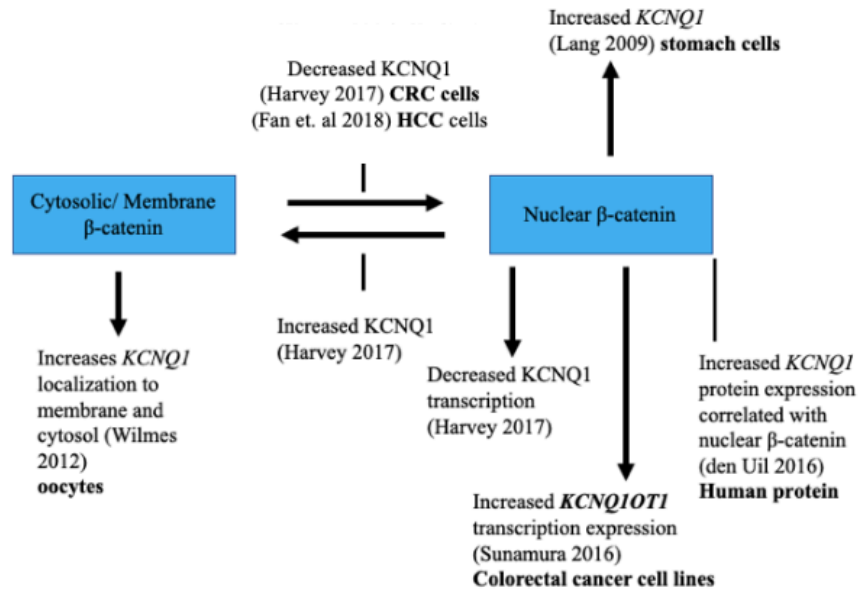


Figure 10: Interactions between *KCNQ1*, β -catenin, and *KCNQ1OT1*.

Identification of Tumor Suppressor CFTR

As described above, *Cftr* was identified as a CIS gene in the same screen as *Kcnq1*. *KCNQ1* export of potassium ions provides the electrical driving force for the

export of chloride ions by *CFTR*. Therefore, *CFTR* was postulated to play an important role in colorectal cancer also.

To test whether *Cftr* may also be a tumor suppressor, *Apc^{Min}* mice were crossed with *Cftr^{F1/F1}* Villin-Cre mice to produce a conditional KO of *Cftr* in the intestinal tract (Than *et al.*, 2016). In *Apc^{+/+}* *Cftr^{F1/F1}* Villin-Cre mice, *Cftr* deficiency alone was sufficient to cause intestinal adenoma tumors in 60% of the population after one year (Than *et al.*, 2016). Organoids were produced from these *Cftr* deficient mice, and clonogenicity was increased significantly when compared to *Cftr* WT organoids (Than *et al.*, 2016). *CFTR* was also examined in human tissue mRNA samples from stage II colorectal cancer patients (Than *et al.*, 2016). Within this cohort, *CFTR* expression was correlated with increased survival rates, solidifying *CFTR*'s role as a tumor suppressor in colorectal cancers (Than 2016).

CFTR, Cystic Fibrosis, and Colorectal Cancer

CFTR, cystic fibrosis transmembrane conductance regulator, is located on chromosome 7q31.2, and encodes a protein which forms a chloride channel in cells responsible for the production mucus, tears, and sweat (NIH, 2019). This chloride channel is extremely important for the regulation of these various fluids (Kleme *et al.*, 2016). *CFTR* is expressed in the respiratory tract and the intestine. Similar to *KCNQ1*, *CFTR* is expressed within the intestinal crypt. *CFTR* is expressed in the respiratory tract, gastrointestinal tract, pancreas, gall bladder, and the spleen (NCBI, 2019).

Cystic fibrosis is a very deadly genetic disease, leading to airway blockages due to mucus build-up (Quinton, 1983). It is the most common autosomal recessive disease

in Caucasians. Of all genetic diseases, cystic fibrosis is responsible for the most deaths among Caucasian populations (Kleme *et al.*, 2016). In 90% of patients, lung disease, often brought on by infections is the ultimate cause of death (Burney & Davies, 2012). It was identified in 1938 by Dorothy Anderson after a heat wave in New York resulted in peculiar cases of lung infection along with extreme salt loss through the sweat (Elborn, 2016). The cause of this disease, improper ion transport due to a mutated *CFTR* protein, was not determined until nearly a half century later (Kerem *et al.*, 1989). Cystic fibrosis is inherited in an autosomal recessive manner, primarily affecting the respiratory system and gastrointestinal tissues (Fuchs *et al.*, 1994). Patients with cystic fibrosis develop serious mucus accumulation and inflammation within their lungs and airways (Elborn, 2016). When *CFTR* is functioning, it allows the movement of chloride into the airway space. Water follows to maintain the ion gradient, and this keeps the mucus layer thin (Rafeeq & Murad, 2017). However, when *CFTR* is not functioning, chloride ions do not move out of the cells, and thus the water does not move into the mucus layer, and the mucus becomes thick and immobile (Rafeeq & Murad, 2017). This abnormal mucus layer provides a highly favorable environment for the growth of bacteria, resulting in serious lung infections (Rafeeq & Murad, 2017). This environment leads to bronchiectasis, a thickening of the bronchi due to inflammation and infection (Elborn, 2016). There are other organs affected by mutations in cystic fibrosis, including gastrointestinal blockages, pancreatic dysfunction, and an ionic imbalance due to excess salt released in the sweat (Rafeeq & Murad, 2017).

Cystic fibrosis patients can have various mutations within the *CFTR* gene, which results in a lack of a mature protein in the membrane (Cheng *et al.*, 1990). There are

more than 2000 gene mutations that have been observed in *CFTR* which can lead to the development of cystic fibrosis (Elborn, 2016). These mutations have been organized into different classes, determined by what functional effect the mutation has on the *CFTR* protein (Elborn, 2016; Burney & Davies, 2012). One mutation, F508del (deletion of the 508th amino acid, phenylalanine), is present in 70% of all cystic fibrosis cases (Rafeeq & Murad, 2017).

Cystic fibrosis patients have an increased risk for colorectal cancer, nearly 5-10 times greater than someone who does not have cystic fibrosis (H'mida Ben-Brahim *et al.*, 2015; Yamada *et al.*, 2018; Maisonneuve *et al.*, 2013). That risk increases for these patients up to 25-30 times a greater risk after an organ transplantation (H'mida Ben-Brahim *et al.*, 2015). To better understand how to treat both cystic fibrosis and colorectal cancer, more must be understood about the regulation of *CFTR*, and its role in the intestine.

Specifically, we wanted to examine how *CFTR* may be interacting with the major drivers of colorectal cancer in the intestinal crypt. Since β -catenin is the most important pathway in the intestinal crypt environment, we chose to investigate the interactions of *CFTR* and β -catenin. As with *KCNQ1*, we would expect a negative correlation between *CFTR* and β -catenin, as β -catenin is a pro-cancer transcription factor and *CFTR* is a tumor suppressor.

Several groups have reported that *CFTR* deficiency leads to increased β -catenin activity in the nucleus (Than *et al.*, 2016; Strubberg *et al.*, 2018; Zhang *et al.*, 2018). This has been reported in murine adenomas and organoid cultures. However, *CFTR* deficiency has also been reported to cause decreased nuclear β -catenin in whole intestinal

lysates (Liu *et al.*, 2016). It has been suggested by Strubberg *et al.*, that the difference may be due to an alteration in *CFTR* activity in the stem cell compartment compared to the whole intestine. However, more information is needed to understand *CFTR* and β -catenin's interactions with each other in the intestinal stem cell compartment.

Gaps in Knowledge

In colorectal cancer, *KCNQ1* and *CFTR* have been established as tumor suppressors, and the low expression levels of these tumor suppressors are indicators of poor prognosis colorectal colon cancers (Liu *et al.*, 2014; Than *et al.*, 2016; den Uil *et al.*, 2016). However, the question of how these tumor suppressors are regulated and their underlying mechanism of action remains a major gap in knowledge. Specifically, their relationship with β -catenin must be investigated. The Wnt/ β -catenin pathway is the most important pathway within the intestinal crypt, as it regulates the crypt environment, determines proliferation rate, and regulates stemness. The relationship between *KCNQ1* and β -catenin, and between *CFTR* and β -catenin is still a convoluted story which needs clarification.

Understanding their activity within the colon stem cell compartment is also of vital importance, as the stem cell compartment is thought to be the site of initiation for colorectal cancer. The majority of data collected in non-cancer models has been done with small intestine. Although small intestine models are a valuable tool for understanding how the crypts and stem cells function, more information is needed to understand the dynamics of the colon intestinal crypts, and whether they differ significantly from the small intestinal environment. This area is a significant gap in

knowledge and more intestinal stem cell work needs to be conducted within colon stem cell models.

Hypotheses

My thesis will address several of these gaps in knowledge. I will first investigate whether β -catenin regulates the expression of *KCNQ1*. I hypothesize that β -catenin down regulates the expression *KCNQ1*. Higher β -catenin expression, during *APC* loss, is associated with development of colorectal cancer. Therefore, we would expect that *KCNQ1* would be down regulated when β -catenin was high. I will investigate this hypothesis using siRNA experiments, luciferase reporter assays and RT-qPCR.

I will also address the mechanism for *KCNQ1* and *CFTR* as tumor suppressors in a stem cell model: colon organoids. The organoids will be harvested from murine colon intestinal crypts, providing valuable information regarding the interactions within the colon stem cell compartment. I hypothesize that *KCNQ1* and *CFTR* may be regulating β -catenin activity within the intestinal stem cell compartment. If so, it may suggest that *KCNQ1* and *CFTR* act as tumor suppressors through their regulation of β -catenin. I will investigate this hypothesis through immunofluorescent staining of β -catenin in colon stem cell organoids.

Chapter 1: Regulation of *KCNQ1* by *KCNQ1OT1* and β -catenin

Materials and Methods

Cell Culture

Colorectal cancer cell lines were obtained from American Type Culture Collection (ATCC). Two cell lines were utilized: T84 and SW480, both adherent. T84 is a colorectal carcinoma cell line, derived from a lung metastasis from a 72 year old male. SW480 is a colorectal adenocarcinoma cell line, derived from a Duke's type B tumor harvested from a 50-year old male patient. Both cell lines were cultured at 37°C in 5% CO₂ in DMEM (Dulbecco's modified Eagle's medium), with 10% FBS and 1% Glutamine. The cells were fed or passaged every three to five days.

For feeding, the existing media was removed from the cell culture flasks, and 4ml of fresh media was added to the cells. For passaging, the old media was removed from the flask, and 2ml of phosphate buffered saline (PBS) was added to rinse the remaining media from the flask. The cells were treated with Trypsin-EDTA (ethylenediamine tetraacetic acid) and incubated for two to three minutes at 37°C in 5% CO₂. After trypsinization, 4ml of media was added back to the flask, to neutralize the trypsin reaction. The cells were moved to a 15ml conical tube and centrifuged at 300xg for 3 minutes. The cells, now in a pellet at the bottom of the conical tube, had the 4ml of media removed from above the pellet using a glass Pasteur pipette connected to a vacuum system. The pellet was resuspended in 2ml of media, and a select dilution was added to 4ml of fresh media in a fresh cell culture flask. The cells were returned to the incubator 37°C at 5% CO₂.

RNA Harvest for RT- qPCR

T84 and SW480 cells were plated at 7×10^5 cells/dish and incubated for 24 hours at 37°C at 5% CO_2 . The cells were harvested for total RNA using the QIAGEN RNeasy Mini Kit (Cat # 74104). The cells were first collected from the cell culture dishes by trypsinization, then resuspended in 1ml of media in a 1.5ml Eppendorf tube, and put on ice. The cells were spun down in a micro centrifuge for 5 minutes at 1,200 rpm at 4°C . All media was removed from the cells, now in a pellet at the bottom of the tube. $600\mu\text{l}$ of RLT buffer was added to the cell pellet to disrupt the cells, and the solution was pipetted gently until the pellet was resuspended. The cells were homogenized 15 times with a 1ml $25^{5/8}\text{G}$ syringe. To precipitate the RNA, one volume of 100% ethanol was added to the sample which was mixed by pipetting. The solution was transferred to a column, and the liquid was drawn through the membrane by centrifugation. The flow through was discarded. The column was treated with a DNase solution to remove DNA in the column. The RNA column was washed with an ethanol buffer, RPE, and spun empty to remove residual ethanol. DNase/RNase free water was added to elute the RNA and measured on a Nanodrop to determine concentration.

siRNA Knockdown of KCNQ1OT1 and β -catenin in SW480 cells

SW480 cells were grown at a concentration of 2×10^5 cells/dish and incubated for 48 hours at 37°C , 5% CO_2 . The cells were transfected with 75ng of a combined solution of four *KCNQ1OT1* siRNAs (Cat# S105393696, S104713625, S104713618, S1036663240), or β -catenin siRNAs (Cat.# S1002662478). A siRNA control, OT3, was

used in all experiments. OT3 is a negative siRNA control: an siRNA without a target sequence. This control is necessary to determine that our effect is due to the specific gene being targeted, and not the presence of the siRNA alone. The cells were incubated at 37°C, 5% CO₂ for 24 hours, after which the cells were collected for RNA harvest.

Reporter Assay Cell Culture

The cell line HEK293 was obtained from American Type Culture Collection (ATCC). HEK293 is an epithelia human cell line isolated from an embryonic kidney. This cell line was kept at 37°C and 5% CO₂ in DMEM (Dulbecco's modified Eagle's medium), with 10% FBS and 1% Glutamine. The cells were fed or passaged every three to five days.

Molecular Cloning

The cloning plasmid pLS-LR was provided by Dr. Matthew Slattery (Figure 15). This plasmid contains an ampicillin resistance gene, a restriction digest site capable of allowing cleaving by Kpn1, Sac1, Mlu1, Nhe1, Xho1, Bg1II, and HindIII. This region is followed by a TK basal promoter, followed by a Renilla SP optimized luciferase gene.

Our inserts of interest were obtained from Integrated DNA Technologies (IDT) with specific restriction digest sites on either end. The cloning plasmid was digested Bg1II and MluI to create the correct sticky ends for cloning. The restriction digest was tested on a gel to assure that the plasmid was successfully cleaved.

Depending on their size, IDT prepared the inserts as double stranded, or single stranded. For cloning, double stranded inserts are necessary. This required the annealing of the single stranded inserts to their complementary base pair matching strand. To

anneal, the single stranded inserts were diluted to 100 pmol/ μ l. 1 volume of Tris-EDTA (TE) buffer was added to the inserts and diluted down to 20pmol/ μ l in TE buffer. 2.5 μ l of each insert solution (forward and reverse strands) were added to 5 μ l of 10X STE buffer, and 40 μ l of water. The tube was placed in a 95 $^{\circ}$ C heat block for 3 minutes. The heat block was unplugged, and the tube slowly cooled to room temperature (RT) overnight. The annealed sample was put at -20 $^{\circ}$ C.

The inserts were ligated into the cloning plasmid pLS-LR (Figure 9). A carefully measured ratio of vector: insert was prepared depending on size of insert. This ratio was determined by use of the New England Biolaboratories ligation calculator. This reaction also contained ligase buffer, T4 DNA ligase, and H₂O. The sample incubated for 30 minutes at RT, and frozen at -20 $^{\circ}$ C.

The plasmids, hopefully with inserts present, were transformed into DH5-alpha *Escherichia coli* (*E. coli*). Colonies were selected and placed in LB (Luria-Bertani) broth, with ampicillin (1:1000). After sixteen hours at 37 $^{\circ}$ C with shaking, allowing for proliferation of the transformed bacteria, the plasmid DNA was isolated with a Qiagen miniprep procedure. To determine whether our insert was present in the plasmid, the DNA was treated with the same restriction enzymes as were used in the initial cloning and run on a gel to determine whether the inserts were present in the samples. RT-qPCR was used to amplify the smaller segments to allow gel visualization.

Luciferase Reporter Assay

HEK293 cells were growth in DMEM media in white 96 well plates at a seeding density of 2,000 cells/ well and incubated at 37 $^{\circ}$ C, 5% CO₂ for 24 hours. The next day

the cell's media was changed to OptiMEM media, transfected with the 75ng of the cloned pLS-LR plasmid, incubate for 24 hours (Figure 11). A control plasmid was also

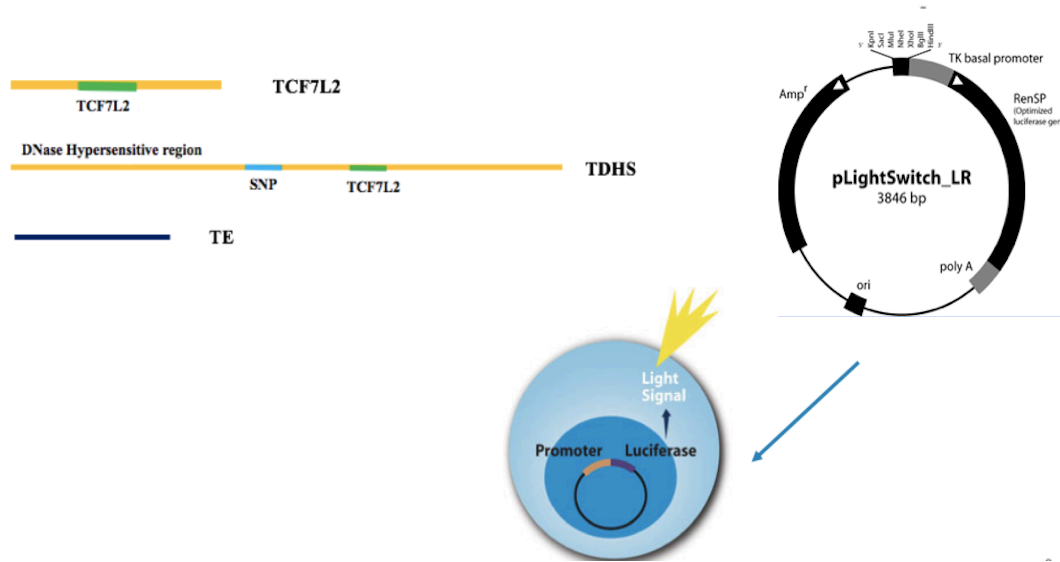


Figure 11: General method for luciferase assay. Sequences cloned into our reporter plasmid. Plasmids are then transfected into cells, wherein the luciferase gene is expressed, Luciferin protein is made, and the resulting light signal is read on a luminometer. SwitchGear Genomics 2017.

transfected into separate wells for normalization. The next day the media was changed to Wnt media or DMEM media, and the cells were again incubated at 37°C and 5% CO₂ for 24 hours. The next day the plate was wrapped in parafilm and frozen at -80°C for 24 hours to induce lysis of cells. The next day, the assay plate was removed from the -80°C freezer half an hour before the start of the luciferase assay. After the allotted 30 minutes, 100X substrate solution diluted 1:1000 in assay buffer was added to the plate, after which the plate was immediately wrapped in tin foil and incubated at RT for another 30 minutes. The plate was read in a luminometer plate reader.

Results

I. Regulation of *KCNQ1* by *KCNQ1OT1*

Comparison of cells lines with altered KCNQ1OT1 methylation patterns

KCNQ1OT1 expression is downregulated by promoter CpG island methylation. To determine if *KCNQ1* was regulated by *KCNQ1OT1* we compared expression in two colorectal cancer cell lines known to be differently methylated: T84 has one unmethylated allele, and SW480 has both alleles are unmethylated (Nakano *et al.*, 2006). Based on our understanding of regulatory relationship of *KCNQ1OT1* on *KCNQ1*, we

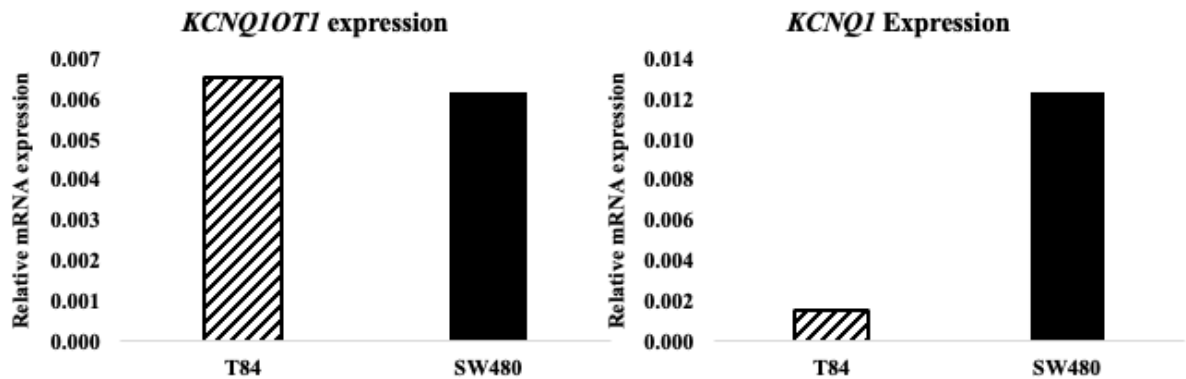


Figure 12: Expression of *KCNQ1OT1* and *KCNQ1*, normalized to 18S. One biological replicate.

expected *KCNQ1* levels to be higher in T84 cells than in the SW480 cells. However, we saw the opposite effect in the *KCNQ1* expression, and there was no difference between the mRNA expression of *KCNQ1OT1* in the two cell lines (Figure 12). This result suggests that factors other than promoter methylation affect *KCNQ1OT1* expression and factors other than *KCNQ1OT1* affect *KCNQ1* expression in these cell lines.

This could suggest that *KCNQ1OT1* expression does not change significantly when there is one allele unmethylated compared to when two alleles are

unmethylated. This suggests that these cell lines are not a good model for examining these gene interactions. It could also suggest that *KCNQ1* expression is not dependent on *KCNQ1OT1* alone.

siRNA KD of KCNQ1OT1

To examine this interaction in another way, we attempted to knockdown the expression of *KCNQ1OT1* using siRNA. We hoped this would demonstrate how the removal of *KCNQ1OT1* expression affected the expression of *KCNQ1*. SW480 cells were transfected with a mixture of four *KCNQ1OT1* siRNAs, and RNA was harvested. We used a non-targeting siRNA, OT3, as a negative control. However, the siRNA

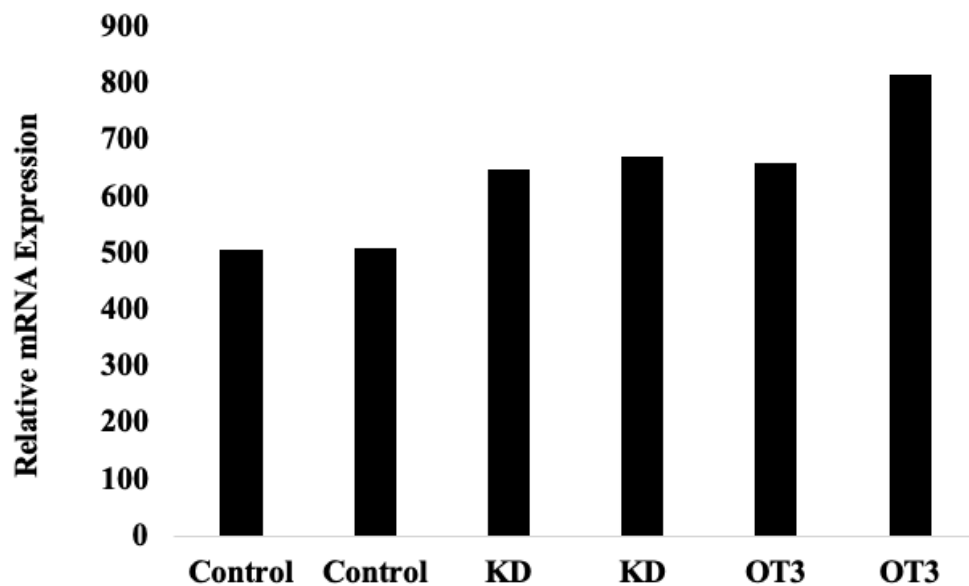


Figure 13: siRNA knockdown (KD) of *KCNQ1OT1* in SW480 cells. OT3 is a non-targeting siRNA control.

knockdown of *KCNQ1OT1* was unsuccessful (Figure 13). siRNAs act primarily in the cytoplasm, while *KCNQ1OT1* has been reported to localize to the nucleus (Pandey *et al.*, 2008). This is probably the reason that the KD of *KCNQ1OT1* was unsuccessful.

KD of β -catenin expression via transfection of siRNA

To explain the interaction between *KCNQ1* and *KCNQ1OT1* more effectively, we next decided to knockdown expression of β -catenin in the SW480 cells. β -catenin directly regulates the expression of *KCNQ1OT1*. When β -catenin expression is low, *KCNQ1OT1* expression is also low (Sunamura *et al.*, 2016). We did an siRNA knockdown of β -catenin in SW480 cells and examined the expression of β -catenin, *KCNQ1*, and *KCNQ1OT1* mRNAs using RT-qPCR (Figure 14). The expression of β -catenin was decreased in the β -catenin depleted samples, as was the expression of *OT1* as reported in the literature (Sunamura *et al.*, 2016). However, the expression of *KCNQ1* was also decreased slightly. This result suggests that either neither *KCNQ1OT1* or β -catenin affects *KCNQ1* expression, or possibly that they have opposing effects. The

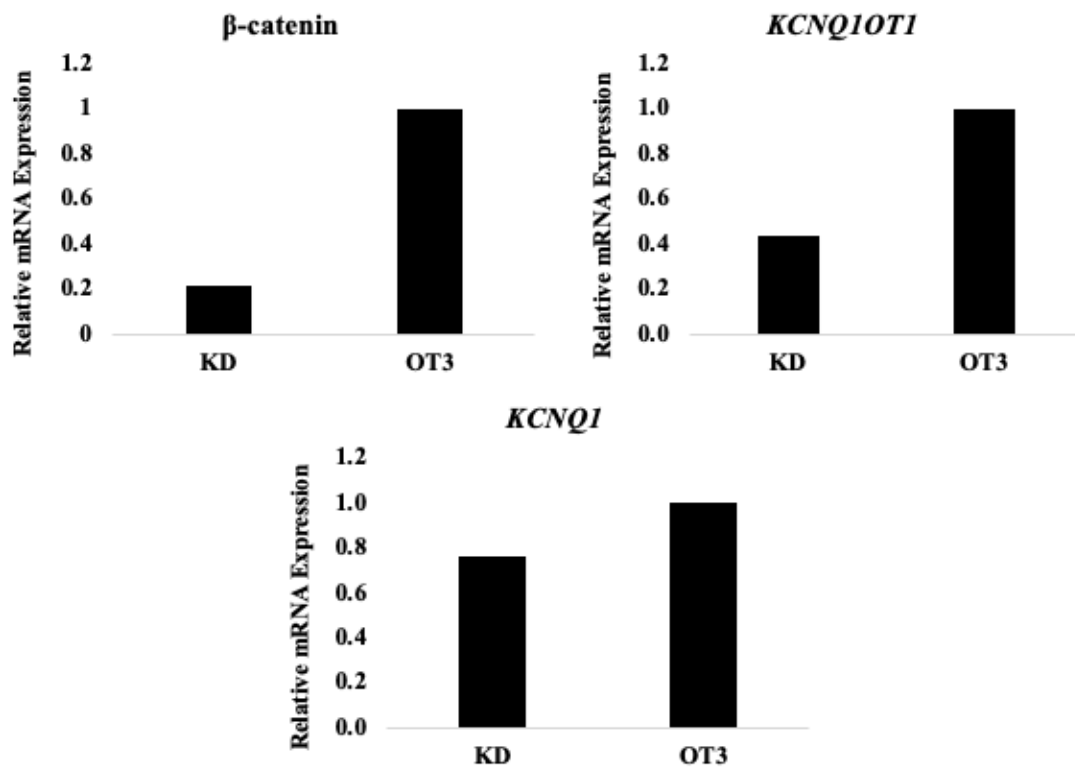


Figure 14: siRNA KD of β -catenin. All gene expression is normalized to 18S. One replicate in SW480 cells.

depletion of β -catenin down regulates and decreases *KCNQ1OT1*, while also decreasing the expression of *KCNQ1*.

II. *KCNQ1* genomic enhancer region

Identification of putative enhancer

To examine *KCNQ1* expression using another approach, the *KCNQ1* genomic sequence was surveyed for eQTLs (SNPs, or single nucleotide polymorphisms) associated with altered expression of *KCNQ1*). This analysis, conducted by Dr. Matthew Slattery, identified SNP rs2283155 in *KCNQ1* intron 2 that was associated with differential *KCNQ1* expression. This SNP was located within a putative enhancer region characterized by DNase hypersensitivity. This SNP could represent a regulatory site itself or more likely, it could be in linkage disequilibrium with another variant that alters *KCNQ1* expression (Figure 15; Dr. Slattery, unpublished). We tested the hypothesis that this region regulates *KCNQ1* expression.

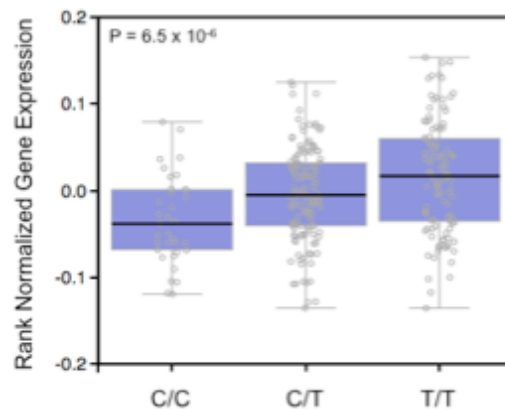


Figure 15: *KCNQ1* expression in individuals separated by genotype at the ICR enhancer SNP. The C allele is associated with low *KCNQ1* expression and the T allele is associated with high expression. Data are based on the thyroid gene expression data from the GTex project (Dr. Slattery, unpublished)

Development of reporter assay

Therefore, to determine whether this putative enhancer region, marked by SNP rs283155 was an active enhancer region within our system, I cloned specific regions of the putative enhancer region (Figure 16) into a reporter plasmid (Figure 17). The reporter plasmid is an established model for determining activity of putative enhancer regions.

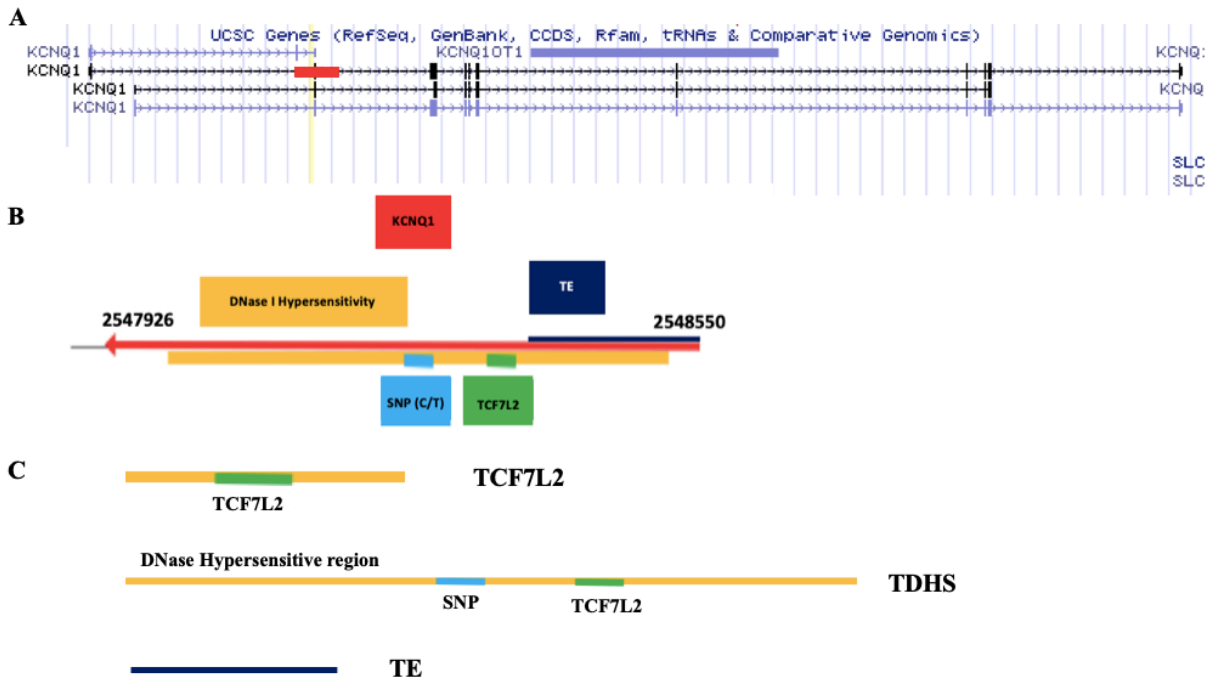


Figure 16: Putative enhancer region within *KCNQ1* intron 2. A) UCSC genome browser readout of *KCNQ1* region and location of SNP. Red box shows general location of enhancer region. B) Map of enhancer region. Red is *KCNQ1* gene. Yellow indicates the DNase I hypersensitivity region (a region that allows greater access by DNase I, indicating an increased accessibility of the chromatin). Blue is the SNP. Green is TCF7L2, the binding site for TCF, a binding partner for β -catenin. TE is the end of the DNase sequence. C) The three sequences that I cloned to test for regulatory activity. UCSC Genebank.

The reporter plasmid contains restriction enzyme cleaving sites followed by a basal promoter, a luciferase gene, the site of origin, and an ampicillin resistance gene. The basal promoter will induce expression of the luciferase gene slightly, low levels of luciferase protein will be made, and there will be a low luciferase signal when

luciferin is added to the cells. If the insert is an enhancer, the luciferase signal will increase, and if the insert is a down regulator, the luciferase signal will decrease. Since this putative enhancer contains a TCF7L2 binding site, and TCF7L2 is the DNA binding

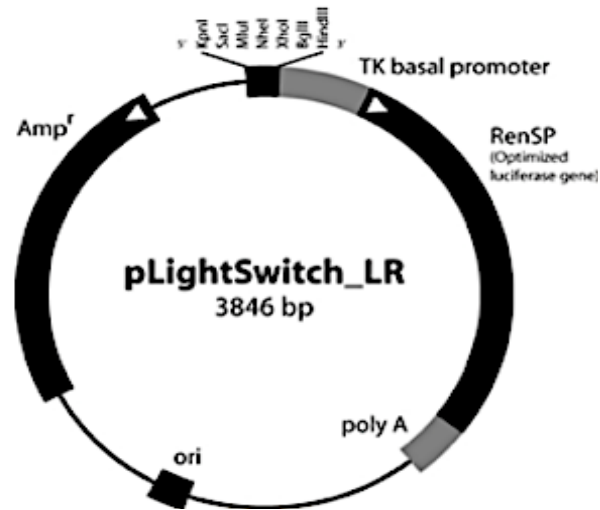


Figure 17: Reporter plasmid pLS-LR. The plasmid contains a basal promoter, and a restriction digest-surrounded region for cloning of the sequence of interest. The luciferase gene, RenSP, allows for detection of enhancer/ regulator activity by the inserted sequence. The plasmid also contains an ampicillin resistance gene, to provide a method by which to select it during the transformation steps. SwitchGear Genomics.

partner for transcriptionally active β -catenin, we decided to examine whether the putative enhancer was active in the Wnt/ β -catenin pathway. We tested this by treating our cells with Wnt, to induce β -catenin activity.

There were several layers of troubleshooting before we got reliable results with the reporter assay. I first tested two different control plasmids: *LDHA* and *NQO1*. *LDHA* is a housekeeping gene encoding a lactate dehydrogenase with moderate to low expression in cells (Tagliafierro *et al.*, 2016). *NQO1* is a gene encoding NADPH quinone dehydrogenase which is highly expressed in cells Gray *et al.*, 2016). I therefore

expected to see the *LDHA* control vector yield lower luciferase expression when compared to the *NQO1* vector. The first attempt of the luciferase assay I included only

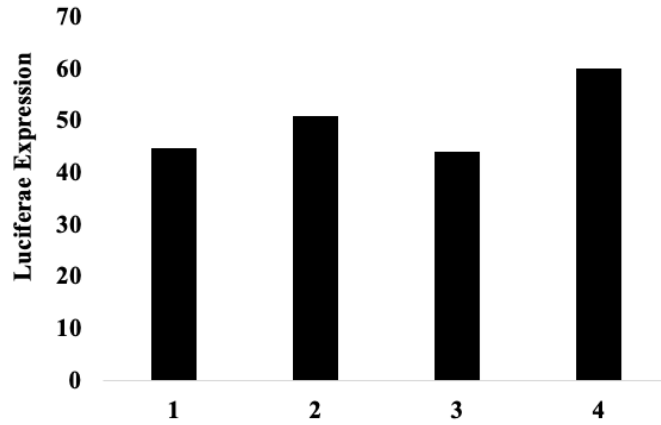


Figure 18: Reporter luciferase assay: *LDHA* control vector luciferase expression in Hct116. Values are averages of ten wells each.

the *LDHA* vector in Hct116 cells, a colorectal cancer cell line. This resulted in in extremely low luciferase expression (Figure 18).

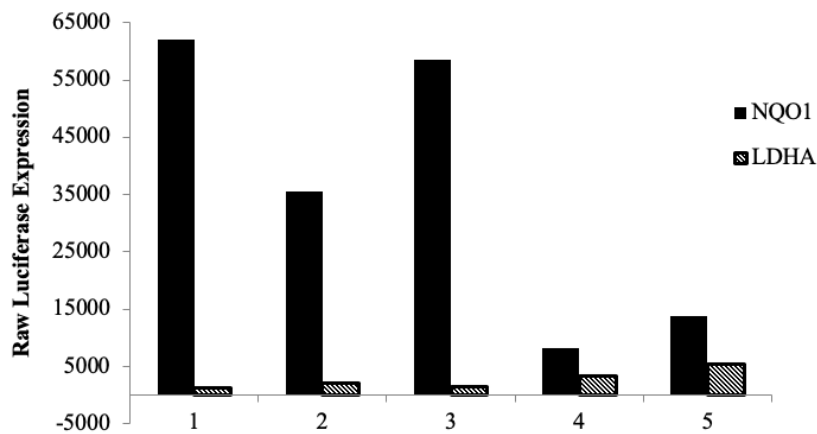


Figure 19: Reporter luciferase assay: NQO1 and LDHA, Hct116. Each number is an individual well.

Since *LDHA* gene expression is known to be low in cells, I also tried *NQO1*, which is known to have higher expression to determine if my low expression of *LDHA* alone was simply due to a constitutively low expression of our cells. *NQO1* did have much higher expression, however, the expression levels were not consistent (Figure 19).

I then began to test my own cloned plasmids, beginning with the TCF7L2 sequence and the TDHS sequences (Figure 16), treated with Wnt and without Wnt. I used the *LDHA* and *NQO1* plasmids as controls. The Wnt-treated samples had extremely

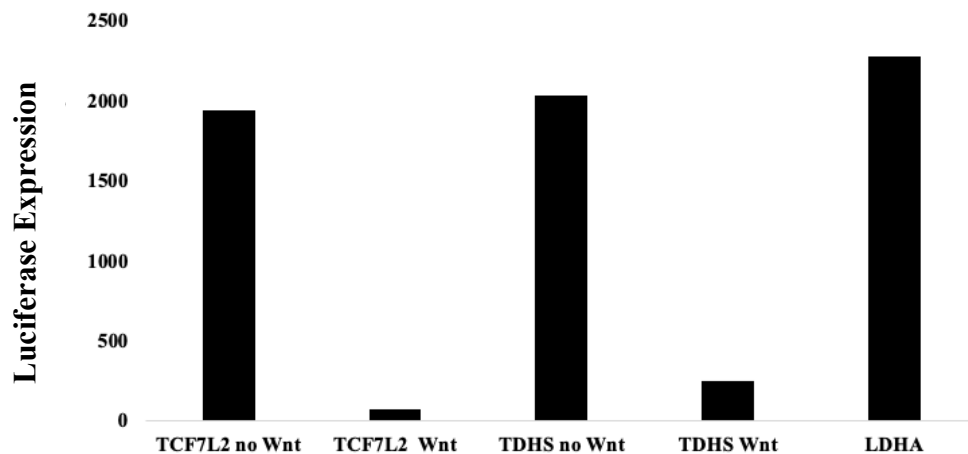
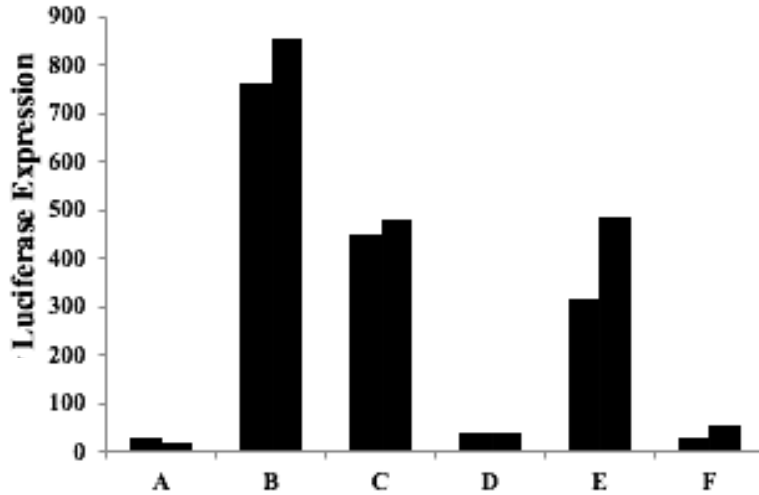


Figure 20: Reporter luciferase assay: TCF7L2 construct compared to TDHS construct with C version of SNP. LDHA was used as a control

low expression compared to the others (Figure 20). I concluded that the Wnt media was interfering with some aspect of the luciferase assay.

Therefore, I set up an experiment with either Wnt-containing media or OptiMEM media at each stage of the assay (Figure 21). After doing this, it appeared that the Wnt media did interfere with the transfection but did not affect the growth phase or the actual

luciferase assay itself (Figure 21). Therefore, I decided to do my transfections in OptiMEM media and change it to Wnt-containing media 24 hours after the transfection.



	Transfection	Growth	Luciferase assay
A	Wnt	Wnt	Wnt
B	Opt	Opt	Opt
C	Opt	Wnt	Wnt
D	Wnt	Wnt	Opt
E	Opt	Wnt	Opt
F	Wnt	Opt	Opt

Figure 21: Reporter luciferase assay: Wnt experiment to determine which stage the Wnt media was interfering with.

Despite transfecting my cells in OptiMEM media instead of Wnt containing media, my following luciferase assays still were not giving me as high yields as I would have expected. I added the optional freezing step which is necessary to lyse all the cells in the wells. Although the luciferase solution in a lysis buffer, freezing makes the lysis step much more effective. Lysis of the cells is necessary to allow to be detected by the luminometer. After I began freezing the plates, I was seeing better luciferase expression (Figure 22).

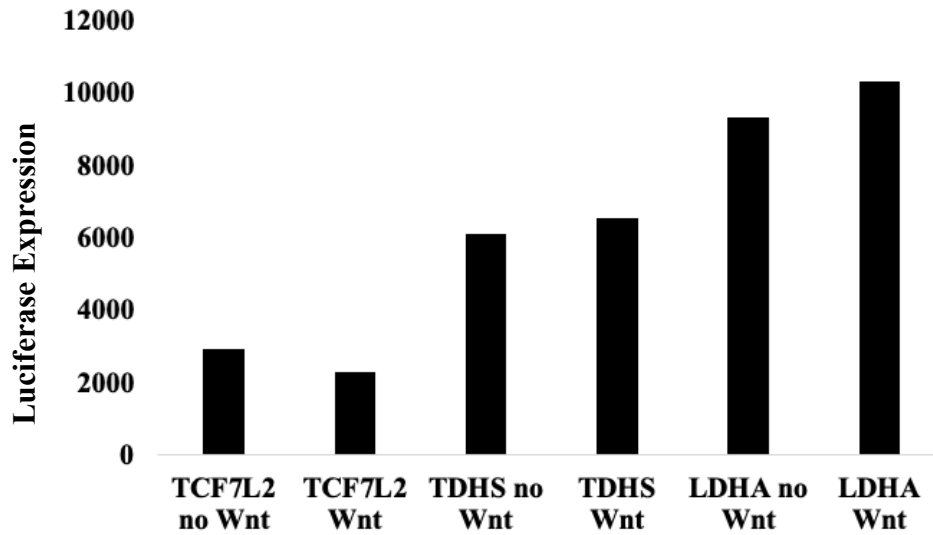


Figure 22: Reporter luciferase assay: Luciferase expression after freezing plate, with TCF7L2 construct and the TDHS construct with C version of SNP. LDHA plasmid is the control. Each was treated with Wnt or no Wnt media

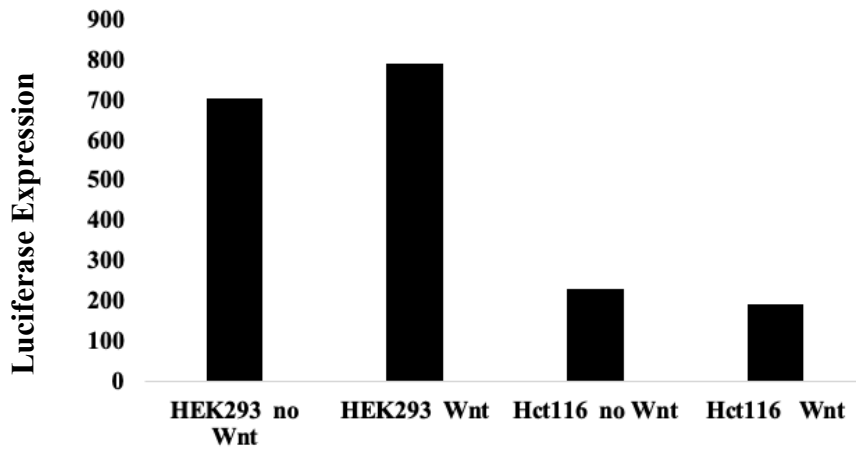


Figure 23: Reporter luciferase assay: Luciferase expression of HEK293 cells and Hct116 cells.

However, I wanted to achieve the highest possible luciferase expression to get trustworthy results. I compared the expression levels of the luciferase assay in HEK293 vs. Hct116 cells. The HEK293 yielded much higher expression values (Figure 23). colorectal cancer cell line; they are an embryonic kidney cell line. However, they 40

have high efficiency for transfections and an active Wnt/ β -catenin pathway (Kim *et al.*, 2008). Therefore, to effectively determine whether our putative enhancer sequence was an active regulator, I decided to continue the rest of my assays with the HEK293 cells.

Evaluation of putative enhancer region

Now that the assay was giving reliable results, I began to examine all my cloned sequences. The first I tried was the TCF7L2 binding site and some surrounding DNA, a construct of 65 bp. This sequence included only the TCF7L2 binding site, as well as a small amount of surrounding DNA (Figure 16). I expected this site to be increased in response to Wnt treatment, as Wnt activates the activity of β -catenin in the nucleus, and therefore, should induce binding of β -catenin at the site of interest, leading to increased expression of our reporter gene. With Wnt treatment, I expected and observed increased luciferase expression in the presence of Wnt (Figure 24).

The next sequence I cloned, TDHS, included the entire DNase hypersensitive region as well as the SNP and the TCF7L2 binding site (Figure 16). I made two separate constructs to test both versions of the SNP. I expected to see a difference in expression of luciferase if this region of DNA is acting as an enhancer or a down regulator of gene expression (Figure 23). The TDHS sequences yielded interesting results. The luciferase expression was increased with Wnt, but less than the TCF7L2 binding site alone. There was no differential expression between two different versions of the SNP.

I also cloned a third sequence, TE, which includes the end of the DNase sensitive region, without either the SNP or the TCF7L2 binding site (Figure 16). This sequence was cloned to check for the regulator activity at the end of the TDHS sequence, and this sequence has no detectable regulatory activity (Figure 24).

Our enhancer region appears to be an active regulator. Interestingly, in the presence of our enhancer, the reporter gene has a smaller increase in expression compared to the TCF7L2 binding site alone. This suggests that our enhancer may have an inhibitory effect.

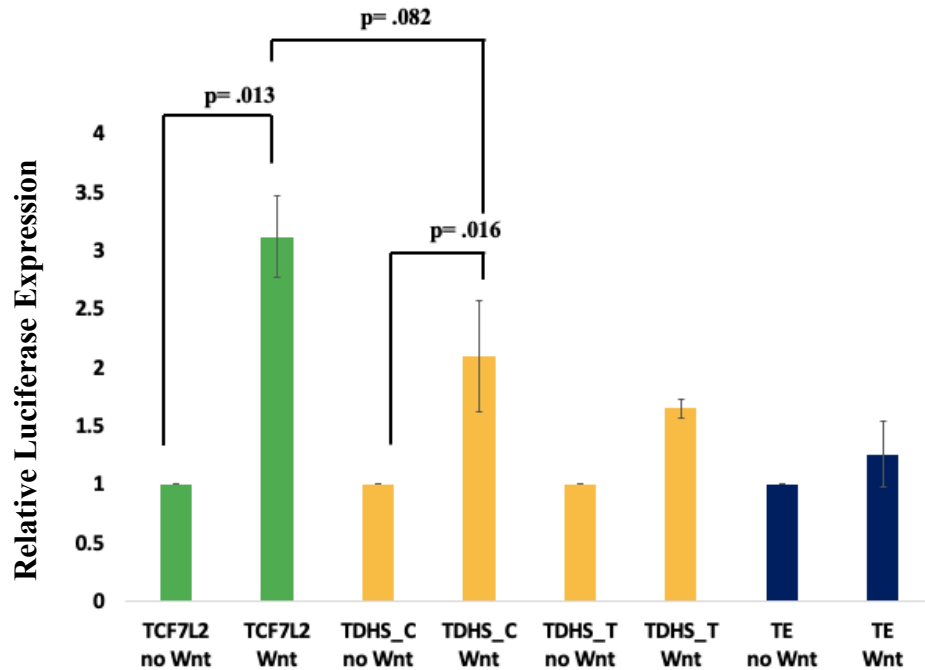


Figure 24: Reporter luciferase assays, with the three sequences of interest molecularly cloned into the pLS-LR vector. Each sample has been treated with Wnt, and a no Wnt control. The values have been normalized to a housekeeping vector, RPL, and then divided by the no Wnt control to determine the ratio between the two. P values were obtained from a 2-tail T-test. Error bars are standard deviation. Two replicates were done for TCF7L2, 3 for each TDHS, and 1 for TE.

Evaluation of enhancer target by RT-qPCR

We next wanted to determine which gene is being regulated by this enhancer region. We hypothesized that this enhancer region was regulating either *KCNQ1* or *KCNQ1OT1* due to its location within the second intron of *KCNQ1*. To test this, I treated HEK293 cells with and without Wnt to replicate the conditions of the reporter assay. I harvested the RNA for RT-qPCR to measure the *KCNQ1* and *KCNQ1OT1* mRNA

expression. I expected that the Wnt treatment would result in an increase of either *KCNQ1* or *KCNQ1OT1*, suggesting that this enhancer region is regulating the expression of that particular gene. Based on my RT-qPCR results, the gene that appears to be regulated is *KCNQ1* (Figure 25). It appears that *KCNQ1* expression matches the expression seen in the reporter assay, with increased expression in the Wnt treatment. I also tested β -catenin, *KCNQ1OT1*, and *CDKN1C*, one of the genes reported to be regulated by *KCNQ1OT1*. β -catenin and *CDKN1C* were not significantly changed between Wnt and no Wnt treatments, but *KCNQ1OT1* was significantly decreased in the presence of Wnt, which was the opposite of what we expected.

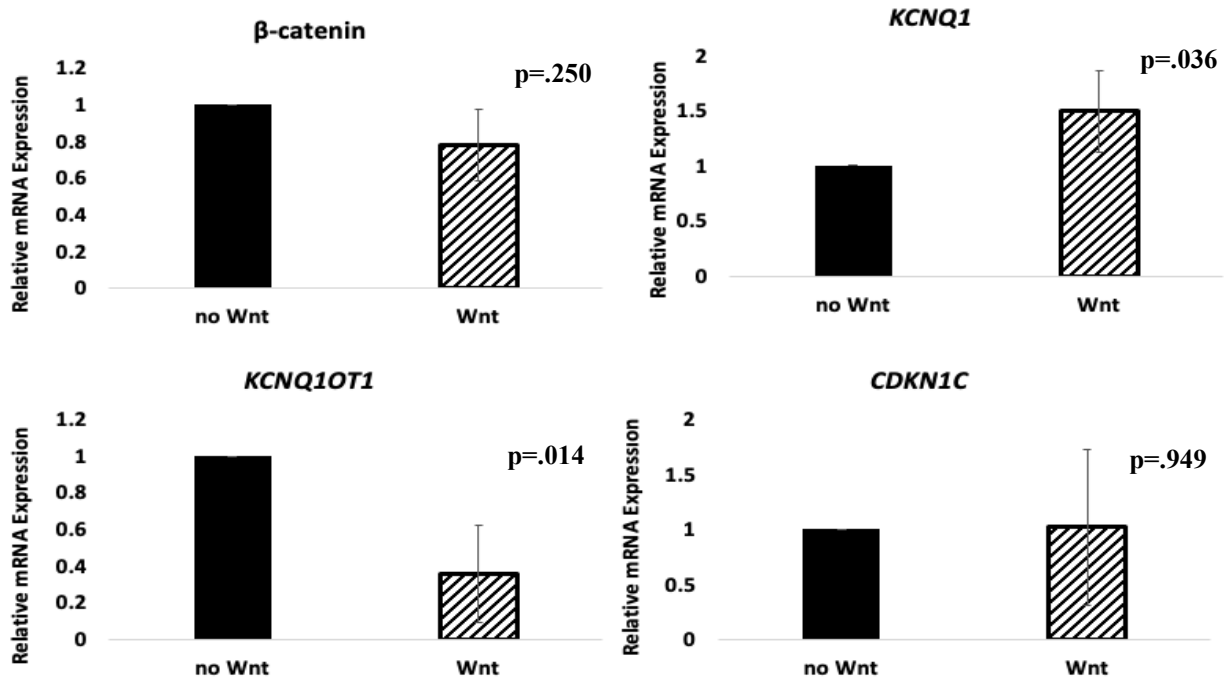


Figure 25: RT-qPCR data from HEK293 cells treated with Wnt and no Wnt media. Each value has been normalized to 18S, and then to the no Wnt control. P values were obtained from a 2-tail T-test. Error bars are standard deviation. 3 replicates.

Evaluation of enhancer target using Hi-C platform

On Dr. Slattery's advice I also used a Hi-C database browser to create virtual 4C (circularized chromosome conformation capture) data to look at the interactions of this enhancer within this gene domain (Figure 26). This browser allows you to input a specific genetic location, and examine the interactions that sequence has with the surrounding DNA. This interaction data is collected by first fixing cellular DNA with formaldehyde. This crosslinks the DNA into its 3D conformation, keeping interacting regions of DNA together (Figure 26). The DNA is then cut throughout with restriction enzymes (Figure 26). This will allow isolation of the crosslinked sections of DNA

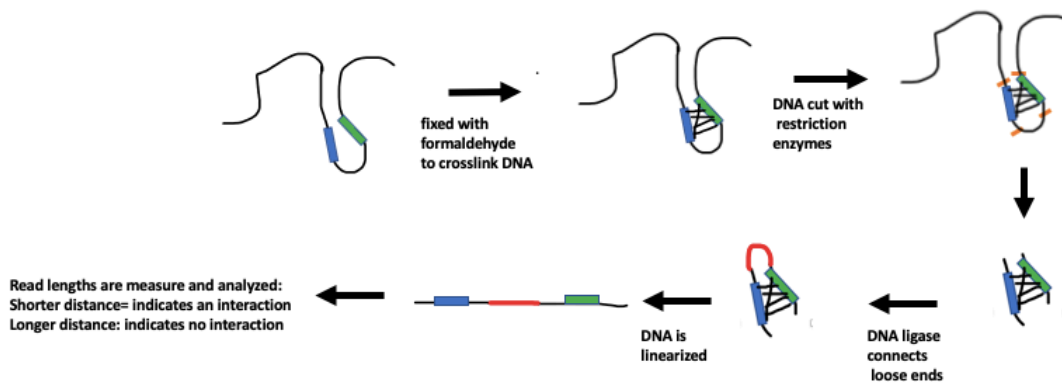


Figure 26: 4C data collection protocol to determine interactions between regions of DNA.

(Figure 26). The crosslinked DNA ends are then connected via DNA ligase, after which the DNA is linearized (Figure 26). The data is then measured and analyzed for read length between cross linked segments: a shorter distance indicates that those two regions are interacting, a longer distance indicates that the two regions are not interacting (Figure 26).

The raw virtual 4C data was generated from HiC data collected in GM12878 cells, a lymphoblastoid cell line. The anchoring point is a 5 kb segment around our 44

enhancer region. The middle peaks are artifacts from the Hi-C assay, as DNA close to the anchoring point will normally have more interactions. The peaks of importance are the ones annotated by the asterisks (Figure 27). This 4C chart suggests that our region of interest is interacting with either the upstream gene region near the *KCNQ1* gene, or the downstream gene region near *CDKN1C*. I saw the same trend in several other cell types including mammary epithelia cells, umbilical vein endothelial cells, lung fibroblast cells, bone marrow lymphoblast cells, chronic myelogenous leukemia cells, and human epidermal keratinocyte cells.

To remove some of the inherent errors from the raw virtual 4C data, such as the central artifact peaks, we generated normalized virtual 4C data, which is thought to be more trustworthy than raw virtual 4C data. The normalized virtual 4C data analyzed with the assistance of Dr. Slattery indicated one main peak of interest, located around 2,900,000 bp (Figure 28). This peak falls within the region of several genes: *CDKN1C*, *SLC22A18*, and *PHLDA2*. All of these genes fall within the *KCNQ1OT1* domain and are thought to be regulated by *KCNQ1OT1* (Higashimoto, Soejima, Saito, Okumura, & Mukai, 2006). *CDKN1C* specifically has been strongly suggested to be down regulated by *KCNQ1OT1* (Chiesa *et al.*, 2012). Therefore, *CDKN1C* mRNA expression was tested using RT-qPCR along with the other genes previously examined: *KCNQ1*, *KCNQ1OT1*, and β -catenin (Figure 25). However, *CDKN1C* expression was not significantly altered in the presence of Wnt. Therefore, *CDKN1C* is not regulated by the Wnt-responsive component of this enhancer but may be regulated by another part of this region.

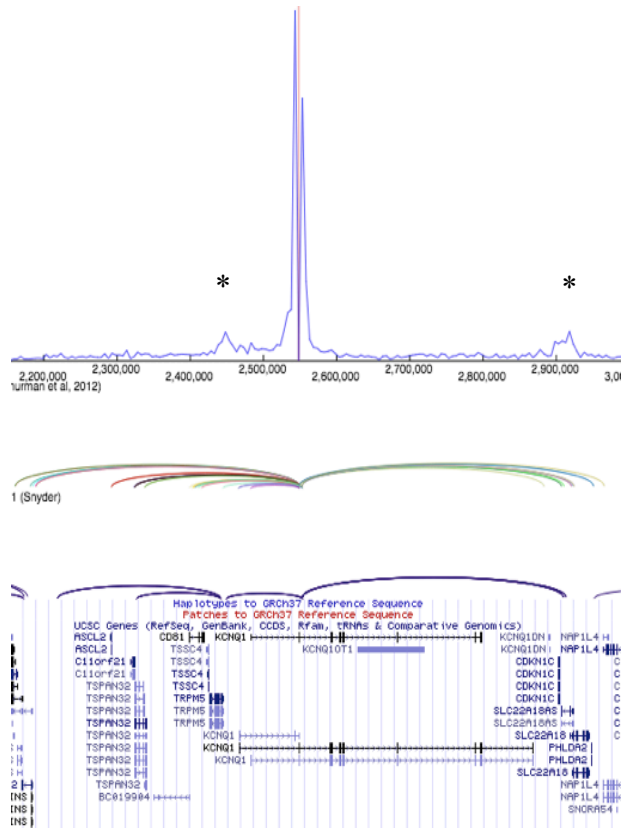


Figure 27: Virtual 4C database readout, raw calculation. Cell line used was GM12878, a lymphoblastoid cell line. X axis is the genome location, Y is the number of number of hits in that particular location.

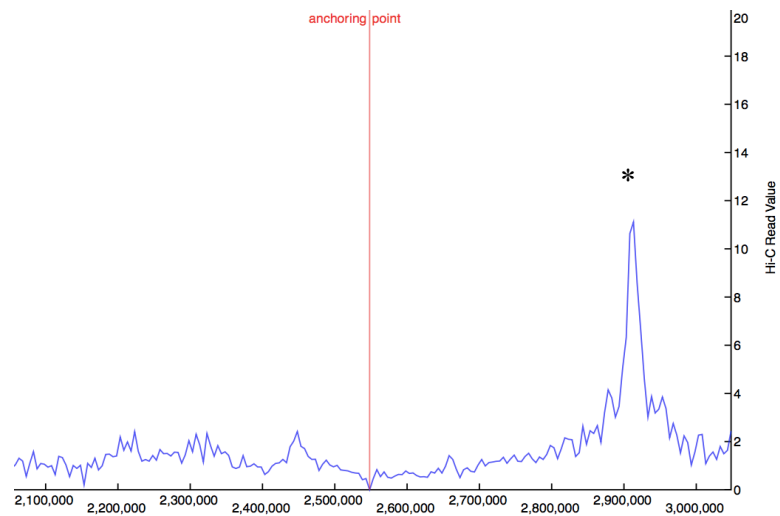


Figure 28: Normalized virtual 4C data generated from GM12878 cells. X axis is the genome location, Y is the number of number of hits in that particular location.

To further attempt to understand the interactions occurring between *KCNQ1*, β -catenin, and *KCNQ1OT1*, I conducted a literature search of Chip-Seq data to determine where β -catenin was known to bind, and if it bound specifically to *KCNQ1* or to *KCNQ1OT1*. However, I found that β -catenin binds to both the promoter of *KCNQ1* and also to *KCNQ1OT1* (Rapetti-Mauss *et al.*, 2017); (Sunamura *et al.*, 2016). Therefore, it appears that β -catenin may regulate both *KCNQ1* and *KCNQ1OT1* expression.

Discussion

Summary

Regulation of *KCNQ1* by *KCNQ1OT1*

There are several conclusions that I was able to make from my experiments investigating the relationship between *KCNQ1*, *KCNQ1OT1*, and β -catenin expression in colorectal cancer cell lines. Based on current understanding of the *KCNQ1OT1* long non-coding RNA from human Beckwith-Wiedemann syndrome data, *KCNQ1OT1* is thought to downregulate the genes within its region, including *KCNQ1* (Valente *et al.*, 2019). However, it has also been suggested that *KCNQ1* expression is independent of *KCNQ1OT1* expression, at least in the developing heart (Korostowski *et al.*, 2012). Therefore, it can be concluded that the expression of *KCNQ1OT1* may be tissue and development-stage specific, and that the downregulation of the genes within this domain is not universal. I sought to try to clarify the role of *KCNQ1OT1* in our system, colorectal cancer. I hypothesized that *KCNQ1OT1* down regulated *KCNQ1*. To test this hypothesis, I compared the gene expression of two colorectal cancer cell lines: T84 and SW480. These cell lines have differential methylation of the *KCNQ1OT1* long non-coding RNA. SW480 has both alleles unmethylated, T84 has one allele methylated and one allele unmethylated. Therefore, I would expect higher expression of *KCNQ1OT1* in the SW480 cells and lower expression of *KCNQ1OT1* in the T84 cells. I also wanted to examine the expression of *KCNQ1* in these two cell lines. If *KCNQ1OT1* down regulates the expression of *KCNQ1*, then I would expect higher expression of *KCNQ1* in the T84 cells, and lower expression of *KCNQ1* in the SW480 cells. However, my results were not as I expected. The *KCNQ1OT1* expression did not appear to be altered between the two

cell lines, and although the *KCNQ1* mRNA expression was different between the two cell lines, the trend was in the opposite direction than the one I had expected: *KCNQ1* expression was low in the T84, and higher in the SW480 cells (Figure 11).

These results tell us that factors other than promoter methylation influence the expression of *KCNQ1OT1* and that factors other than *KCNQ1OT1* influence the expression of *KCNQ1*.

To look directly at the role of *KCNQ1OT1* I used siRNA in SW480 cells. However, the knockdown of *KCNQ1OT1* was unsuccessful (Figure 11), probably because the cytoplasm-acting siRNAs were not able to reach and successfully knockdown the expression of nuclear-localized *KCNQ1OT1*. It is also possible that the *KCNQ1OT1* siRNA oligos were not targeting *KCNQ1OT1* accurately.

Therefore, we tried to deplete *KCNQ1OT1* expression by knocking down β -catenin. β -catenin has been reported to promote *KCNQ1* expression in colorectal cancer cell lines and siRNA knockdown of β -catenin has been used experimentally to knockdown expression of *KCNQ1OT1* in these lines.

Knockdown of β -catenin in colorectal cancer cell line SW480 yielded the same results. β -catenin was effectively depleted. *KCNQ1OT1* expression was diminished confirming that in these cell lines β -catenin promotes *KCNQ1OT1* expression. However, *KCNQ1* expression remained unchanged (Fig 14). This result may indicate that neither *KCNQ1OT1* or β -catenin affects *KCNQ1* expression in these cell lines or that that these two factors have opposing effects with *KCNQ1OT1* downregulating and β -catenin upregulating expression.

***KCNQ1* putative enhancer region**

An unbiased examination of *KCNQ1* genomic sequence identified a putative enhancer region in intron 2. This enhancer of 614bp contains a SNP that shows differential *KCNQ1* expression that falls in a DNase hypersensitive region. This region also contains a TCF7L2 binding site. Therefore, I hypothesized that this region might mediate Wnt/ β -catenin regulation of *KCNQ1* expression. To test this hypothesis, I evaluated the enhancer activity of this region and elements of it using a luciferase reporter assay. I created four reporter constructs: TCF7L2, TDHS-C, TDHS-T, and TE which were transiently transfected into HEK293 cells. After treatment with Wnt or vehicle control, cells were evaluated for luciferase activity. The TCF7L2 binding site construct showed the strongest upregulation of luciferase signal in response to Wnt.

The full-length construct, TDHS, with either SNP polymorphism also showed a strong response to Wnt, however this response was ~30% lower than that of the TCF7L2 site alone. The region downstream of the TCF7L2 site showed no response. These results indicate the enhancer region is an active regulatory site that mediates Wnt/ β -catenin signaling. However, the full-length region appears to contain an additional site that inhibits this signaling (Figure 24). *KCNQ1OT1* lies with the *KCNQ1* gene and elements in *KCNQ1* intron 2 are reported to regulate *KCNQ1OT1* (Asahara *et al.*, 2015). Further, if β -catenin was found to upregulate *KCNQ1OT1* this might explain the downregulation of *KCNQ1* in poor prognosis colorectal cancer.

Therefore, I investigated whether our putative enhancer region regulated *KCNQ1* or *KCNQ1OT1*. Analysis of gene expression in HEK293 cells (the cell line used for the reporter assay) treated with Wnt or vehicle control showed that Wnt treatment promoted

transcription of *KCNQ1* but not *KCNQ1OT1* in these cells and so the reporter assay reflects upregulation of *KCNQ1* by Wnt/ β -catenin signaling. There was no increase in β -catenin transcripts presumably because Wnt signaling acts primarily to stabilize β -catenin protein.

To look at enhancer interactions in an unbiased fashion I carried out an *in silico* analysis of chromatin interaction using the Hi-C database to create a virtual 4C map. 4C data maps the interactions between a certain anchor site within DNA, in this case the 5kb region surrounding our enhancer and other genes by crosslinking the interacting DNA (Figure 25, 26). This allowed me to obtain a prediction of where this enhancer region was interacting within the *KCNQ1* and the *KCNQ1OT1* domain.

The normalized virtual 4C data had a high number of hits in one main location: a region downstream of our enhancer region, near the gene *CDKN1C*, a gene downregulated by *KCNQ1OT1*, which encodes a cyclin-dependent kinase inhibitor (Higashimoto *et al.*, 2006). This region also included the genes *SLC22A18*, and *PHLDA2* which are also downregulated by *KCNQ1OT1*. However, Wnt treated HEK293 cells did not show upregulation of *CDKN1C*. The Hi-C data were obtained from GM12878 not colorectal cancer cell lines. However, these results support the hypothesis that this enhancer region is involved in transcriptional regulation of *KCNQ1OT1* targets in a non-Wnt-dependent fashion.

Conclusions

I initially set out to test the hypothesis that *KCNQ1* was down regulated by *KCNQ1OT1*. I was not able to directly test this idea, and I did not uncover any evidence

supporting this.

However, two different studies provided suggestive evidence that Wnt/ β -catenin promotes *KCNQ1* expression. First, data shown in Figure 14 show that decreased levels of *KCNQ1OT1* fail to cause an increase in *KCNQ1* levels when β -catenin is depleted suggesting that β -catenin may promote *KCNQ1* expression in this context. Second, evaluation of a novel putative enhancer indicates that this enhancer also promotes *KCNQ1* expression via Wnt/ β -catenin signaling. However, the physiological significance of these findings remains to be determined.

Chapter 2: *Kcnq1* and *Cftr* effect on β -catenin activity

Examining β -catenin localization in organoid 3D cultures

Materials and Methods

Colon Organoid Preparation

Mice were euthanized according to IACUC specifications with CO₂. After the mouse was confirmed dead by toe pinch, the abdominal cavity was opened by pinching the skin between two fingers, making a V-shaped cut, and pulling apart to rip the skin away from the peritoneum. This was repeated with the peritoneum in the same manner to reveal the intestines. The colon was removed by removing fat and mesentery tissue and cutting below the cecum and just above the anus. The colon was washed in PBS before processing.

The colon was cut longitudinally using special intestine scissors that have one blunt end, to avoid tearing the intestine. This blunt end was inserted into the colon and the intestine was cut open. The colon was washed in a petri dish with PBS and repeated with a fresh PBS containing petri dish. The colon was sectioned into small pieces, small enough to be pipetted in a 10ml pipette, using a razor blade, and transferred into a 50ml conical tube containing 10ml ice cold PBS.

The colon was washed in this 10mls of ice-cold PBS by pipetting up and down three times using a 10ml pipette, first coated with BSA to prevent sticking of the intestinal pieces to the inside of the pipette. After three washes, the pieces were allowed to settle for ten- thirty seconds, and as much PBS as possible was removed from the conical tube. The tube was then refilled with another 10ml of PBS, and this wash step was repeated twenty times. The purpose of this step is to dislodge all single cells and

debris, while keeping the crypts attached to the intestinal pieces. To loosen the crypts from the intestinal pieces, the tissue pieces were resuspended in 25ml of Chelation Buffer with 125 μ l of EDTA and put on a rotator for 70 minutes at 4°C. The tissue pieces were allowed to settle, and the supernatant was removed. 10ml of Chelation buffer was added to the intestinal pieces, and the entire volume was pipetted up and down three times with a strong pipette, to induce mechanical shearing of the tissue. After the pieces settled, 10 μ l of the Chelation buffer (which should contain crypts) was placed on a slide to count the number of crypts present in each wash. Each wash step with crypts was saved in a new 50ml conical tube. This wash step was repeated until approximately 50ml of washes had accumulated, or until crypts were not present when wash buffer was observed under the microscope.

To prepare crypts for plating in Matrigel (growth factor reduced, phenol red free; BD Biosciences), the crypt-containing Chelation buffer was centrifuged at 300xg for five minutes at 4°C. The supernatant was removed using a glass Pasteur pipette connected to a vacuum system. The crypt pellet was resuspended in five to 10ml ADF (Advanced DMEM F12) media, with 1X Glutamine, 1X HEPES. The crypt solution was counted on a hemocytometer: 20 μ l of media was placed on the grid portion of the hemocytometer without a coverslip present. The crypts were counted, and calculations were done to determine volume of crypt solution needed to have a concentration of 3,000 crypts/ row of six wells.

The organoid solution necessary for my chosen concentration was placed in a new 15ml conical tube, and centrifuged at 300xg for five minutes, at 4°C. The supernatant was removed, and placed on ice, with previously thawed Matrigel. The crypt pellet was

resuspended in 80µl of ADF and 120µl of Matrigel. The resuspended crypts were plated quickly onto a pre-warmed 24 well tissue culture treated plate and let incubate at 37°C at 5% CO₂ for twenty minutes, to allow matrigel to harden. 500µl ADF media (with organoid supplements: HEPES, L-Glutamine, RSPO1, EGF, Noggin, B27, N2, N-Acetylcysteine, and Primaxin) was added to each well, and plate was placed back in incubator.

Passaging Organoids

To dissolve the matrigel, 500 µl cell recovery solution (Corning, Cat. No. 354253) was added to each well. After one hour, the matrigel was scraped off the bottom of the plate using a 1000µl pipette tip. The cell recovery solution, now containing organoids and any undissolved matrigel, was transferred to a 15ml conical tube and 10ml of ADF media (without organoid supplements) was added to the tube and well mixed. The organoids were centrifuged at 300xg for five minutes at 4°C. The supernatant was removed via vacuum and resuspended in 1ml media. A 2ml pipette was attached to a 10 µl pipette tip, and the organoid solution was pipetted up and down fifteen times to break organoids up into smaller pieces. The organoid solution was centrifuged once more at the same settings, and the supernatant was removed. The organoids were plated in Matrigel as done before.

Immunofluorescent Cytochemistry for Organoids

This protocol was adapted from the paper Immunofluorescent staining of mouse intestinal stem cells (O'Rourke *et al.*, 2016). Organoids were passaged, and plated in a FluoroDish (World Precision Instruments, Cat. No. FD35-100) and incubated at 37°C at

5% CO₂ for 24 hours in Wnt-free media (Figure 29). The organoids were fixed in 4% paraformaldehyde (PFA) in PME buffer for twenty minutes. The PFA was removed, and the organoids were rinsed in 200μl IF buffer (.2% Triton X-100, .05% Tween), then twice in 200μl ice cold PBS. 200μl permeabilization buffer (1% saponin, 1% Triton X-100 in PBS) was added to the organoids and let incubate for twenty minutes at RT. The permeabilization buffer was removed, and the organoids were again rinsed twice in 200μl ice-cold PBS (Figure 29).

The organoids were prepared for the antibody step by blocking with 200μl blocking buffer (5% BSA, .5% gelatin, .05% Tween in PBS) for one hour at room temperature. The blocking buffer was removed and 40 μl β-catenin antibody (Alexa Fluor 488 Mouse anti- β-catenin, Cat# 562505) (1:9, antibody: blocking buffer) was added to the organoids. The organoids were kept from light at 4°C overnight (Figure 29).

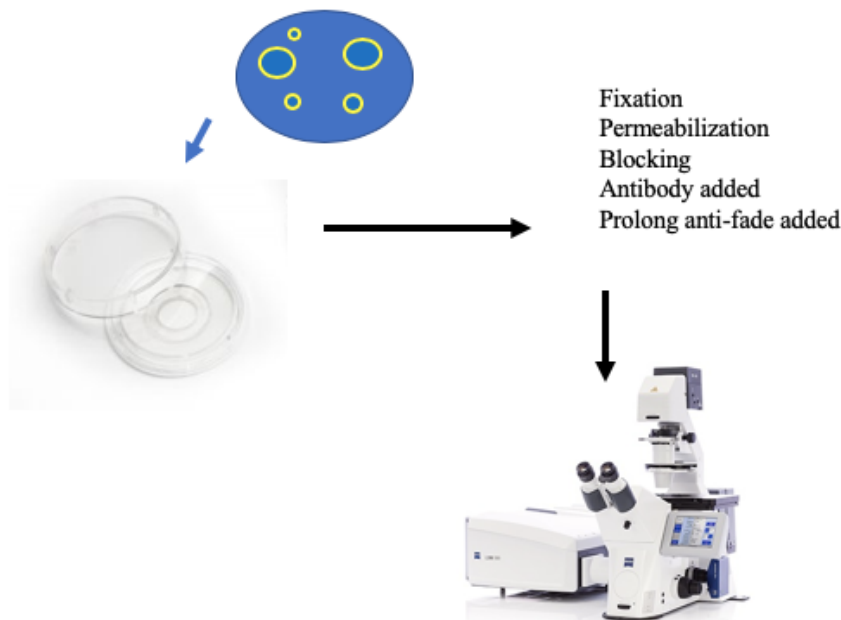


Figure 29: Immunofluorescent staining protocol for 3D organoid cultures.

The antibody was removed, and organoids were rinsed three times in ice cold PBS. Each wash was kept for five minutes each. 30 μ l of 1 μ g/ml DAPI nuclear stain was added to the organoids, and they were incubated in dark for twenty minutes. DAPI was removed, and organoids were rinsed with IF buffer, and all liquid was removed. The organoids were rinsed with MillQ water, and all liquid was removed using the edge of a Kimwipe. A coverslip was then coated with a thin layer of Prolong Gold Antifade (P36930, Thermo Fisher) and placed carefully onto of the organoids on the bottom of the Fluorodish. The organoids were incubated overnight at 4 $^{\circ}$ C, and imaged on a LSM 710 confocal microscope the next day (Figure 29).

A coverslip was then coated with a thin layer of Prolong Gold Antifade (P36930, Thermo Fisher) and placed carefully onto of the organoids on the bottom of the Fluorodish. The organoids were incubated overnight at 4 $^{\circ}$ C, and imaged on a LSM 710 confocal microscope the next day (Figure 29).

Analysis of Nuclear β -catenin in organoids

To analyze the expression of nuclear β -catenin, I circled each nuclei using ImageJ software, and identified each as a region of interest. The nuclei localization was determined via the DAPI signal. I measured the mean intensity of DAPI in each nuclei. I switched to the other channel which had the β -catenin signal and measured the mean β -catenin intensity within each same region of interest. I divided each nuclei's β -catenin signal by the DAPI signal to normalize between organoids. Each nuclei ratio was then averaged, yielding one value per organoid, and approximately 5-7 organoids were measured for each treatment group. These values were again averaged, and the KO value was then divided by the WT value to get an overall ratio representing the difference

between the KO and WT organoids. Three biological replicates were done for each, and 2-tailed T-tests were utilized to determine significance.

Results

Because of the importance of Wnt- β -catenin signaling in colorectal cancer development I evaluated the effect of *Kcnq1* and *Cftr* deficiency on this signaling pathway. To examine the role of β -catenin within the complex stem cell microenvironment, I decided to look at β -catenin activity in stem cell compartment organoid cultures. Translocation of β -catenin from the cytoplasm to the nucleus is a key regulatory step in transcriptional activation. Therefore, I devised a way to measure and quantify the amount of β -catenin within the nucleus of the colon organoids, to better understand how *Kcnq1* and *Cftr* affect β -catenin activity.

Protocol development

It is not practical to analyze protein expression in organoids because of the limited amount of material available, so I developed a quantitative immunocytochemistry method. However, because organoids are large 3D structures many layers of troubleshooting were required to develop this protocol for our lab. This protocol development was done in collaboration with Dr. Cara Hegg of the Whiteside Institute for Clinical Research.

Initial attempts using DAPI to stain nuclei resulted in collapsed organoids (Figure 30). My protocol at this point involved plating the organoids in Fluorodishes, fixing them immediately, and proceeding with the permeabilization, blocking, and treatment with DAPI for nuclear staining. We hypothesized that organoids might be losing their structure due to stress from being plated and then immediately fixed and treated. Adding a 24 hour incubation period after plating the organoids before fixation helped the

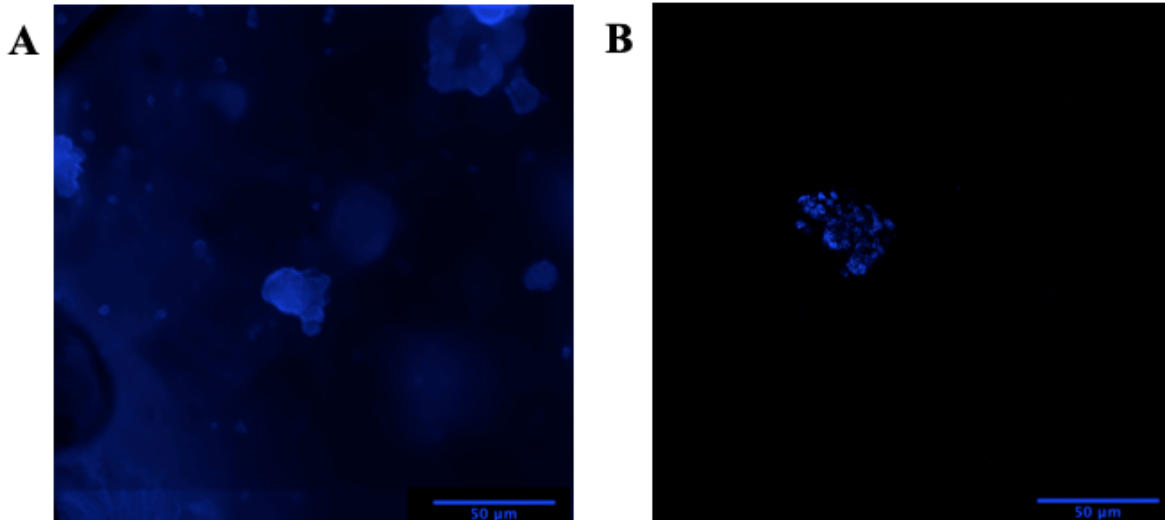


Figure 30: A) First attempt of IFC staining of organoids. Too much DAPI was used, but the loss of spheroid structure is evident. Magnification is 10X. B) Less DAPI was used for next attempt, but again spheroid structure was lost during procedure. Magnification is 25X. Scale bars are 50μm

organoids maintain their structure throughout the fixing and subsequent treatments.

Organoids treated in this way appeared much healthier and maintained a more spherical shape (Figure 31).

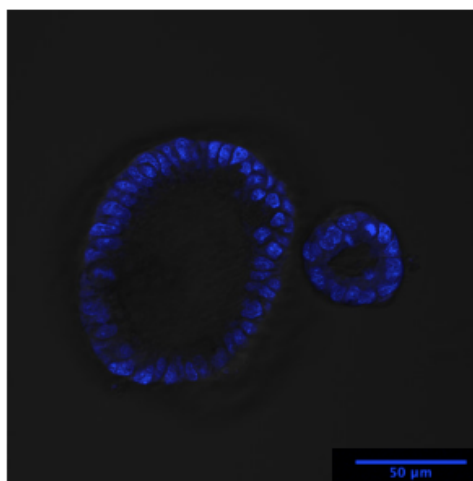


Figure 31: Organoids fixed 24 hours after plating. Spherical shape is maintained. Magnification is 40X. Scale bars are 50μm.

Next, I wanted to optimize the DAPI stain in the organoids, as DAPI nuclear staining did not appear uniform throughout the organoid with a DAPI treatment of 2 minutes. However, DAPI staining appeared to be uniform in a time range from 2 to 30 minutes (Figure 32).

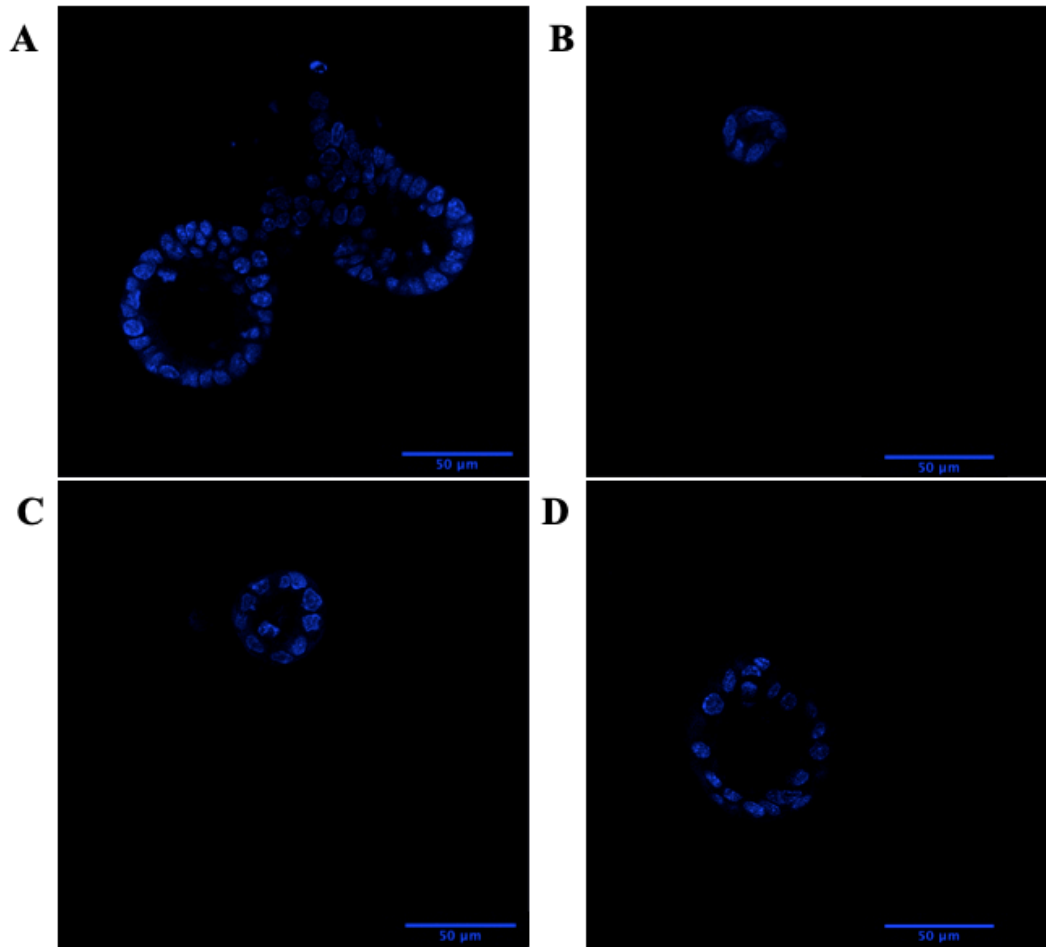


Figure 32: Optimization of DAPI staining time A) 2 minutes of DAPI treatment. B) 8 minutes of DAPI treatment. C) 16 minutes of DAPI treatment. D) 30 minutes of DAPI treatment. DAPI appears to be staining equally well from 2 minutes up to 30 minutes. Magnification is 40X. Scale bars are 50µm.

Once the organoids were maintaining their structure throughout the immunofluorescent protocol, I developed the conditions for β -catenin signaling. To specifically detect nuclear localized β -catenin organoids treated with Wnt-conditioned

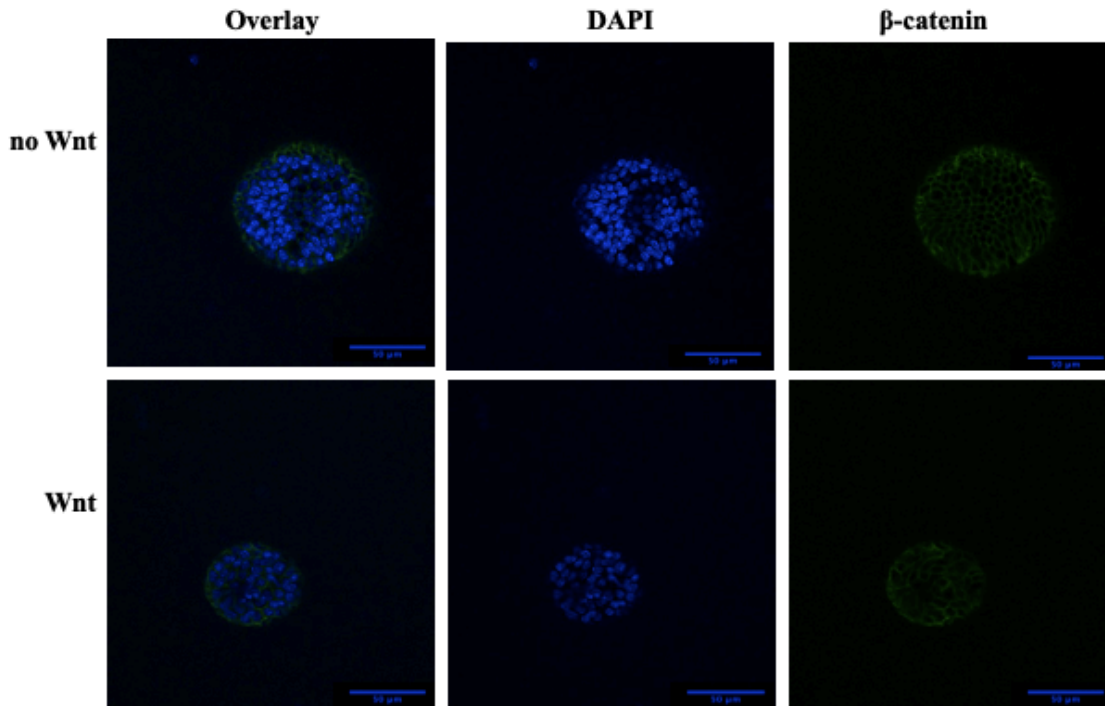


Figure 33: First attempt of staining the organoids with β -catenin. Organoids were treated with media containing Wnt conditioned media or no Wnt media. Although DAPI staining appears strong, the β -catenin antibody does not appear to staining strongly, and no β -catenin is visible in the nucleus in the presence of Wnt as I expected. Magnification is 40X. Scale bars are 50 μ m.

media were compared to untreated controls. In initial experiments the β -catenin signal was weak and no nuclear staining was detected. (Fig. 33)

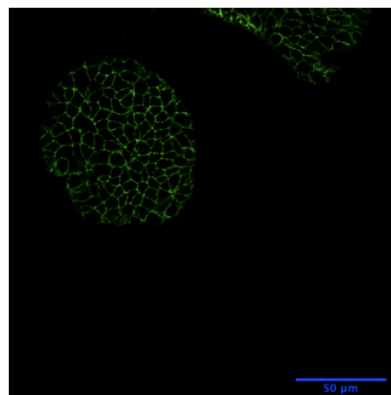


Figure 34: Organoids treated with new saponin permeabilization step. Magnification is 40X. Scale bars are 50 μ m.

To address this problem, I increased the concentration of the permeabilization agent (Triton-X100) and added a second detergent, saponin, to my permeabilization buffer. This improved the β -catenin signal (Figure 34). To develop a control with more

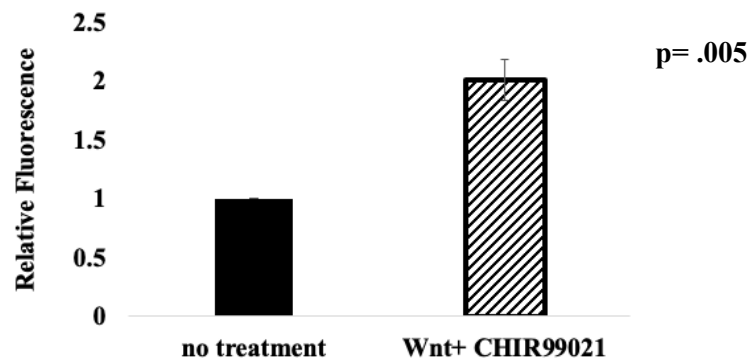
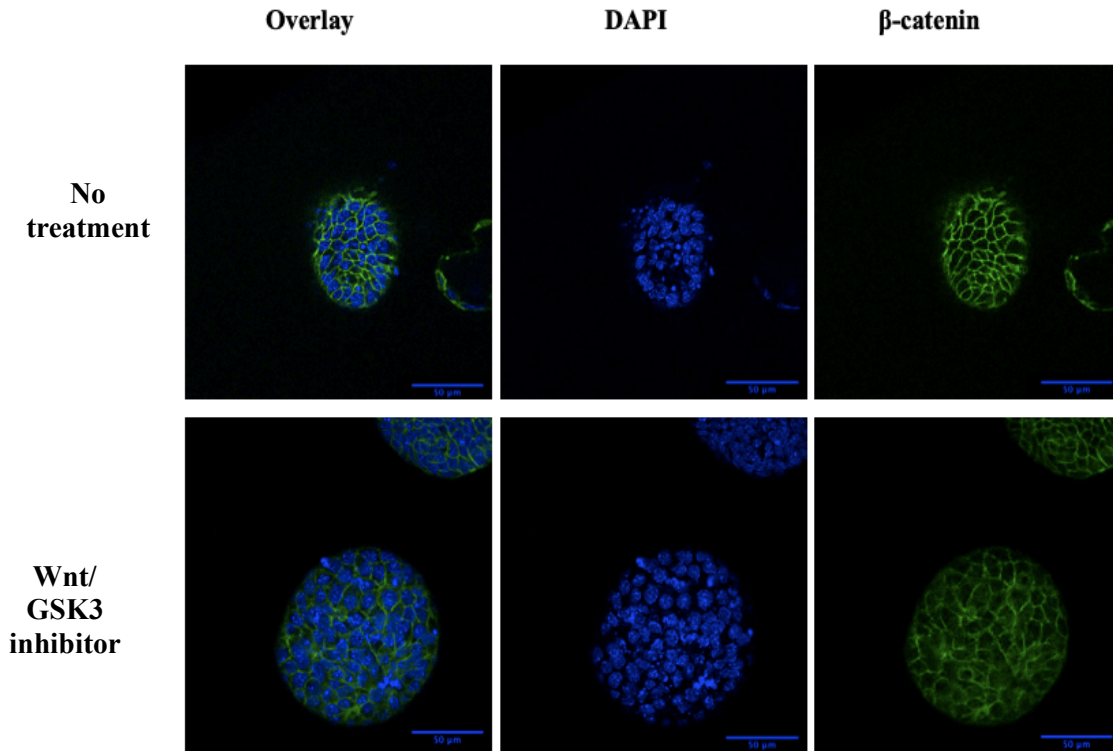


Figure 35: Organoid with no treatment for control. Organoids treated with Wnt containing media and GSK3 inhibitor CHIR990221. With this treatment, a significantly higher amount of nuclear β -catenin is observed. Three replicates were done, p value was obtained from a two tailed t-test. Magnification is 40X. Scale bar is 50 μ m.

robust nuclear signaling I treated organoids with Wnt and a GSK3 inhibitor, CHIR99021 (Sigma, SML1046). GSK3 is a member of the complex involved in cytoplasmic destruction of β -catenin, preventing its translocation into the nucleus (Figure 4). As expected, the nuclear β -catenin was detectable (Figure 35).

However, as *Apc* is known to be one of the key regulators of β -catenin in colorectal cancers, I wanted to establish that our protocol would detect the movement of β -catenin into the nucleus of the organoids with a lack of *Apc*. Therefore, I used organoids generated from mice developed by Dr. Cormier containing a conditional homozygous *Apc* deletion (*Apc^{F1/F1}*) a conditional Luciferase reporter gene (*LSL-Luc*) and a tamoxifen inducible Cre recombinase (CreERT2). Kyle Anderson generated organoids were from uninduced mice. Loss of *Apc* and activation of luciferase were induced by tamoxifen treatment. To verify that *Apc* excision was successful luciferase signaling was visualized (Figure 36). Nuclear β -catenin localization was significantly increased in the *Apc* low organoids compared to the *Apc* high organoids (Figure 37).

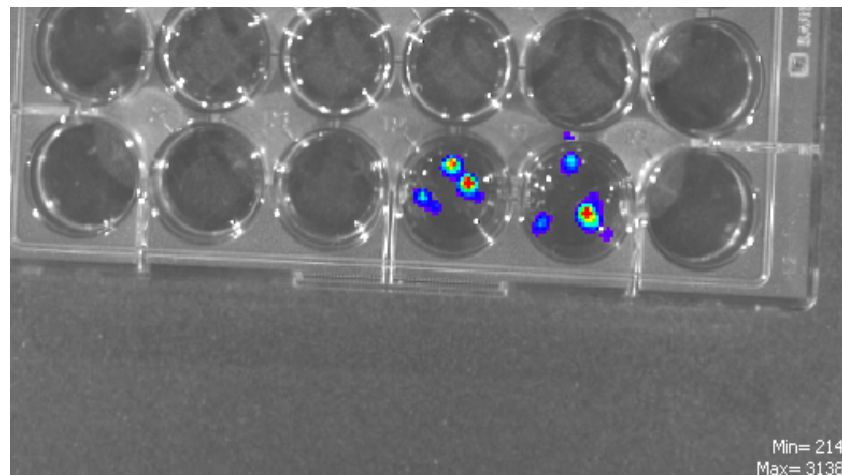


Figure 36: 2 wells of mutated organoids, treated with tamoxifen to induce *Apc* KO. Organoids are expressing luciferase indicating that they have been successfully mutated and are indeed *Apc* KO.

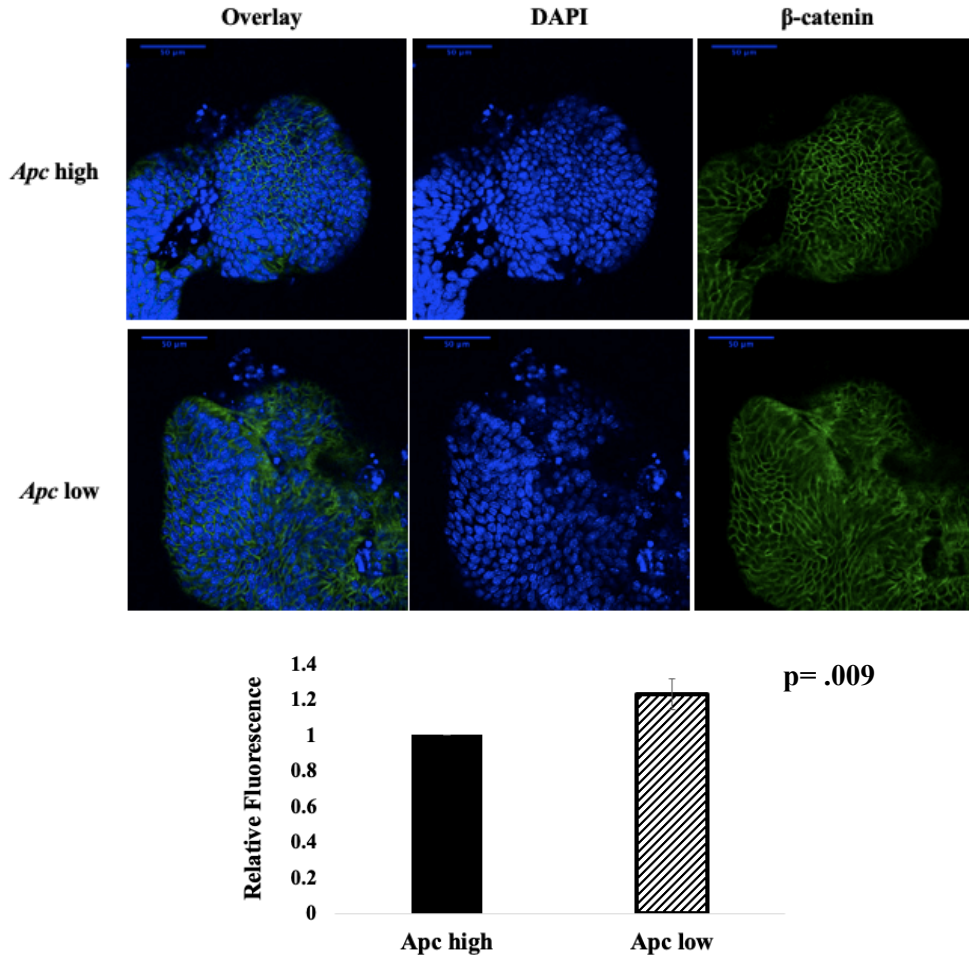


Figure 37: Nuclear β -catenin in *Apc* low and *Apc* high organoids. Nuclear β -catenin is significantly higher in *Apc* low organoids compared to the *Apc* high organoids. Three replicates, p value obtained from a two tailed t-test. Magnification is 40X. Scale bar is 50 μ m.

Examining β -catenin localization in organoid 3D cultures

Now that I had established that my protocol detects nuclear β -catenin with treatments that should induce this localization, I began testing our *Cftr* KO and WT organoids, as well as the *Kcnq1* KO and WT organoids to determine localization of β -catenin with and without these tumor suppressors present.

As *Cftr* and *Kcnq1* are tumor suppressors: lower *Cftr* and *Kcnq1* expression is associated with poor patient prognosis. Therefore, I would expect that with low *Cftr* and *Kcnq1* expression nuclear β -catenin would increase.

The *Cftr* and *Kcnq1* organoids were treated for 24 hours without Wnt before fixing and staining. Organoids isolated from colons are dependent on β -catenin for survival and are maintained in Wnt-containing media. Therefore, as we wanted to look at the basal β -catenin differences between the two, we removed the β -catenin from both before fixing to allow for any differences present to be detected. The *Cftr* and *Kcnq1* organoids yielded expected results. I observed an increase in nuclear β -catenin expression in the *Cftr* KO organoids (Figure 38). I also observed a statistically significant increase in nuclear β -catenin in the *Kcnq1* KO organoids compared to the WT organoids (Figure 39). These data suggest that *Kcnq1* and *Cftr* regulate β -catenin activity. This could potentially be the mechanism by which *Kcnq1* and *Cftr* act as tumor suppressors. This is the only data done in a colon system, providing a very biologically relevant model for understanding the regulation of β -catenin in the colon.

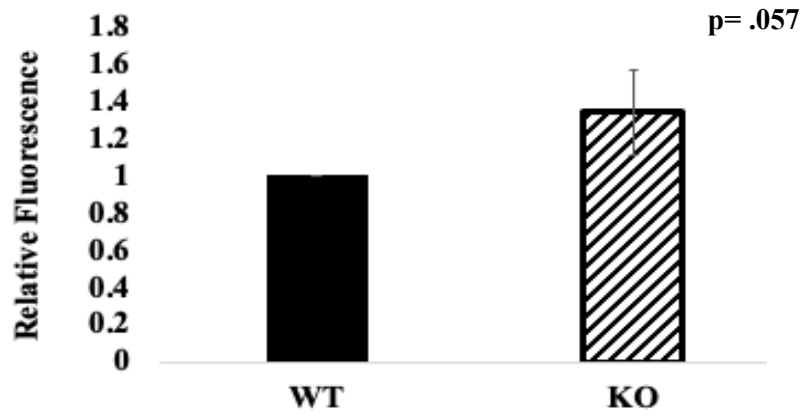
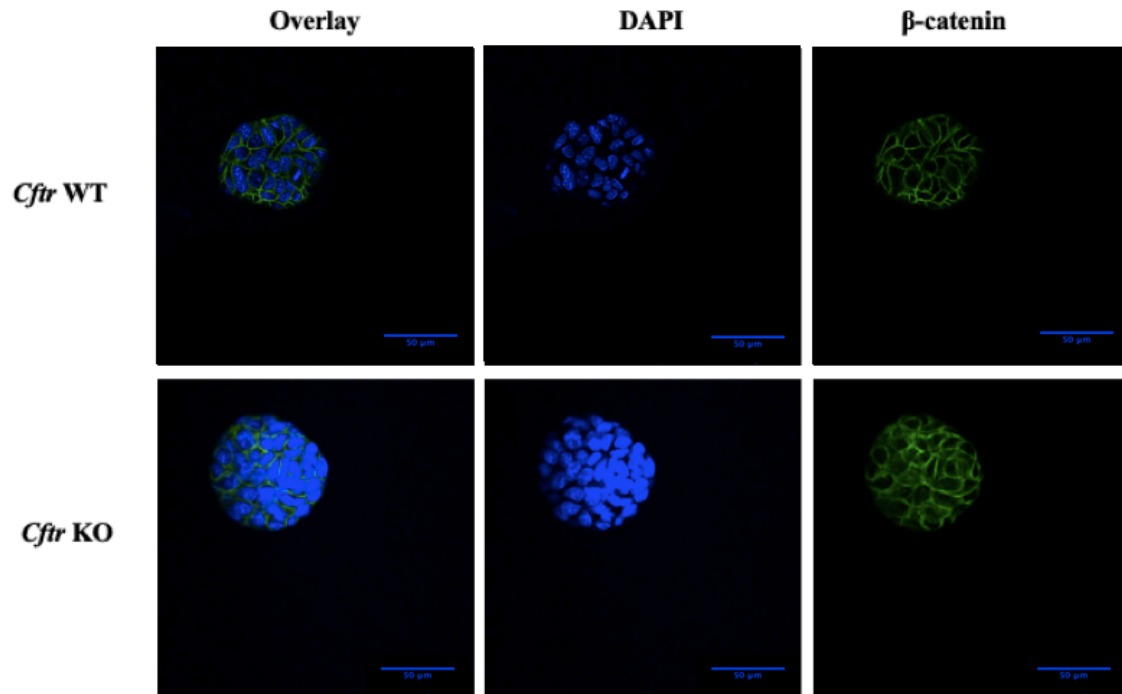


Figure 38: Organoids with high *Cfr* and low *Cfr* expression. Values are relative nuclear β -catenin, normalized to DAPI signal. p-value is from 2-tailed t-test. Magnification is 40X. Scale bar is 50 μ m.

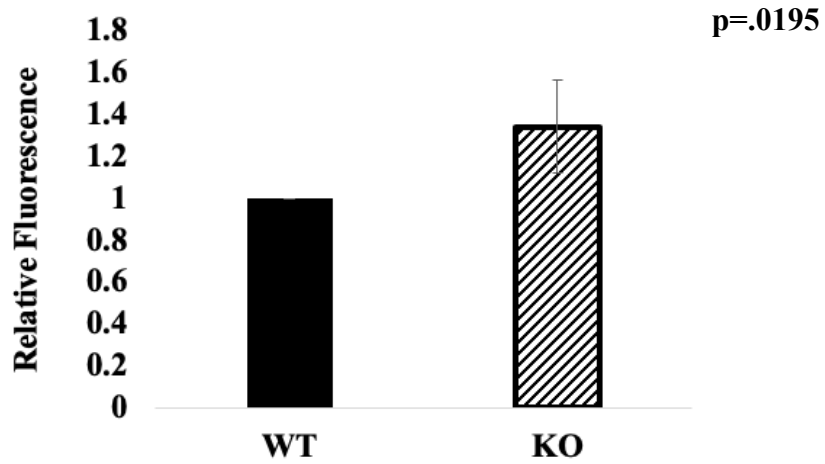
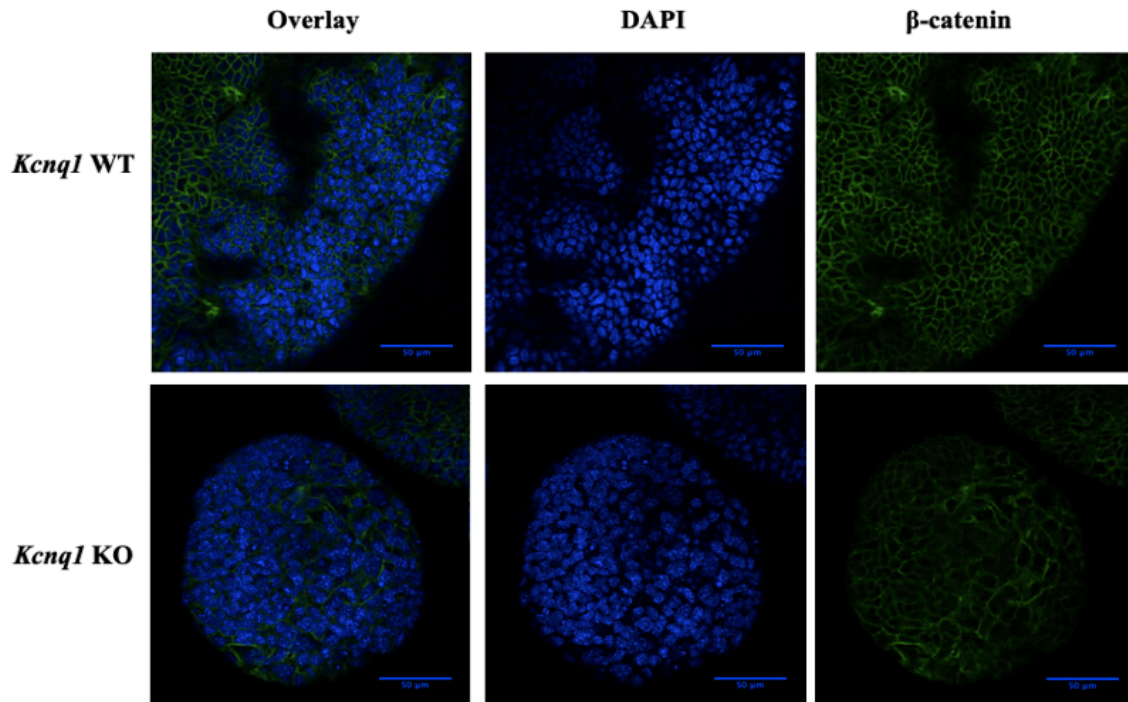


Figure 39: Organoids with high *Kcnq1* and low *Kcnq1* expression. Quantification values are relative nuclear β -catenin, normalized to DAPI signal. p-value is from 2-tailed t-test. Magnification is 40X. Scale bar is 50 μ m.

Discussion

Summary

Because of the importance of the Wnt/ β -catenin pathway in colorectal cancer I wanted to determine if *Kcnq1* or *Cftr* played a role in this pathway. Immunofluorescent analysis of *Cftr* KO organoids revealed increased nuclear β -catenin compared to the WT organoids. The immunofluorescent staining of *Kcnq1* KO organoids with β -catenin revealed significantly increased nuclear β -catenin compared to WT. It suggests that *Kcnq1* and *Cftr* may act as tumor suppressors through their regulation of β -catenin activity. As β -catenin is one of the major drivers of colorectal cancer, this is an important observation.

Our research was done in an organoid system. As *Cftr* and *Kcnq1* are both expressed in the intestinal crypt base, the site of the stem cell compartment and the site of origin for colorectal cancer, looking at these factors in organoids is biologically significant. Much of the research done on *Kcnq1* and β -catenin and *Cftr* and β -catenin has been done in cell lines. Cell lines are not necessarily an accurate model for colorectal cancer due to their 2D structure and monoclonality. They are transformed and typically derived from cancer tumors. Our organoids have many advantages compared to cell lines. Organoids provide a 3D model of cell structure, creating a more accurate representation of the cellular microenvironment. Organoids are heterogeneous, with stem cells and other cells forming a spheroid with a lumen at the center. The organoids are also a non-transformed cancer model, proving an accurate model for basal interactions

within the stem cell compartment. Therefore, our data in organoids is relevant to the question we are trying to address.

These results help to address the question of how *Cftr* activity affects the nuclear localization of β -catenin in the normal colon epithelium which may be relevant for the development of colorectal cancer. Our results are consistent with previous work in which *Cftr* deficiency correlated with increased β -catenin transcriptional activity in small intestinal adenomas (Than *et al.*, 2014) and crypts and organoid cultures (Strubberg *et al.*, 2018). There has also been a report of *Cftr* deficiency associated with decreased β -catenin transcriptional activity (Lui *et al.*, 2017). The discrepancy may be due to the fact that this study measured activity in whole intestinal tissue (Strubberg *et al.*, 2018). Our data is the only data in colon organoids which is very biologically relevant and will add clarity to the question of interactions between *Cftr* and β -catenin in the intestinal stem cell compartment (Figure 40).

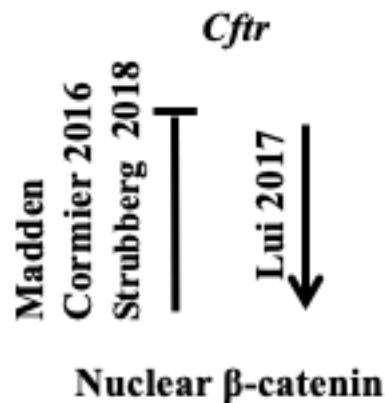


Figure 40: Interactions between *Cftr* and β -catenin in intestinal models including my organoid data.

These results also address the question of how *Kcnq1* activity affects the transcriptional activity of β -catenin. Our results demonstrate that *Kcnq1* deficiency promotes nuclear localization of β -catenin however the mechanism is unknown (Figure 41). Harvey and colleagues report that *KCNQ1* promotes the membrane sequestration of beta catenin (Harvey *et al.*, 2017). It remains to be determined if release of β -catenin into the cytoplasm is sufficient for increased nuclear localization.

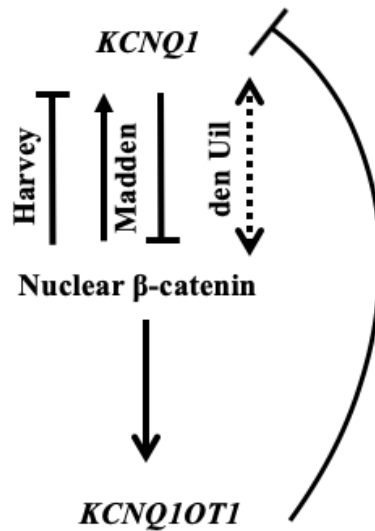


Figure 41: Interactions between *KCNQ1*, *KCNQ1OT1*, and β -catenin in intestinal models, and my data from organoids and the reporter assay

Conclusions

Cftr and *Kcnq1* appear to regulate β -catenin activity. This suggests a mechanism for the tumor suppressor role of *Cftr* and *Kcnq1* in the intestinal stem cell compartment. Our results were obtained in colon organoids, which is a novel system for these observations, and arguably the most biological relevant one for the study of the basic

interactions in the colon. Studying these interactions in a non-cancer model is important in the study of colorectal cancer, to more fully understand the basic mechanisms at play within the intestinal stem cell compartment before cancerous mutations occur.

Appendix

Introduction

The unfolded protein response, activated by the presence of unfolded proteins within the ER, induces three pathways (Grootjans *et al.*, 2016). When a protein is misfolded, the binding immunoglobulin protein (BiP) dissociates from IRE1-alpha, or the misfolded protein may bind IRE1-alpha directly (Figure 42). This induces the splicing of XBP1u (unspliced X-box binding protein), resulting in the activation of XBP1s, transcription activators (Figure 41). These transcription factors activate proteins to assist with protein folding, as well as ERAD (ER-associated degradation) protein, which assists in the degradation of misfolded proteins from the ER (Figure 42). The second pathway is induced when a misfolded protein binds the PERK protein, inhibiting eIF2- α (eukaryotic translation initiation factor 2 α). PERK also induces the movement of transcription factor ATF4 into the nucleus, where it activates expression of genes for anti-oxidant

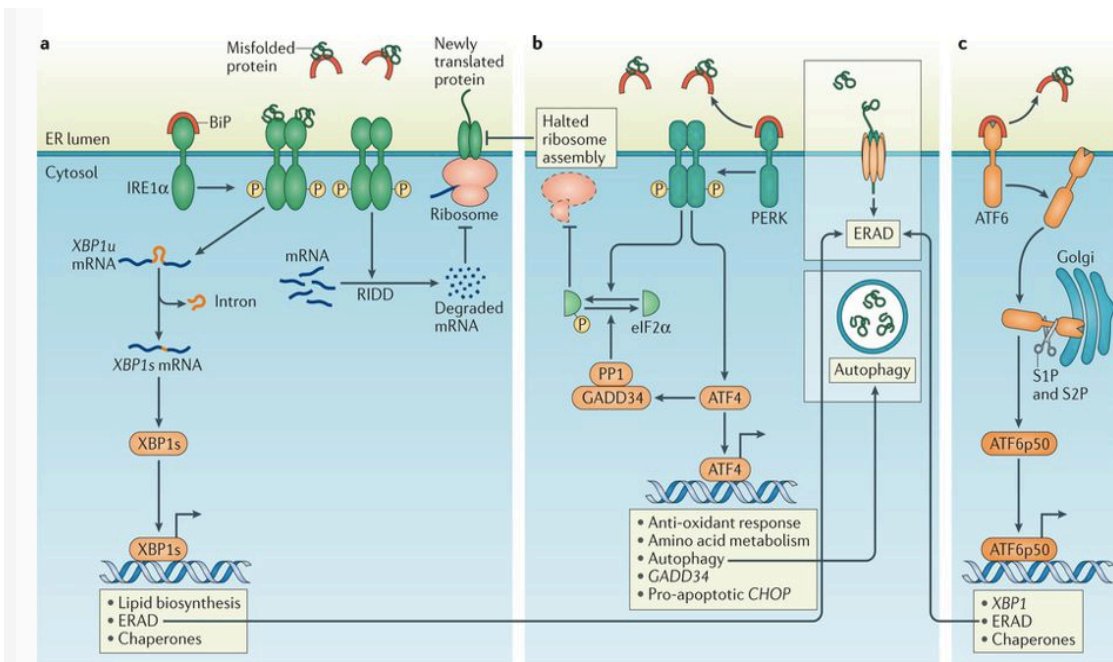


Figure 42: Unfolded protein response, demonstrates the three pathways initiated in the presence of misfolded proteins (Grootjans, Kaser, Kaufman, & Blumberg, 2016).

response, apoptosis, and autophagy (or self-eating: a mechanism wherein a cell destroys organelles or other cellular components (Grootjans *et al.*, 2016). The third pathway involves binding from the misfolded proteins to a factor called ATF6, inducing the movement of transcription factor ATF6p50 to the nucleus, where it induces the expression of XBP1, ERAD, and more chaperone proteins (Grootjans, *et al.*, 2016). The unfolded protein response helps the cell to cope with ER stress produced by unfolded proteins, and this remains an important area of research in the field to better understand the role of *CFTR* within the cell microenvironment.

Materials and Methods

The colorectal cancer cell line Caco2 was obtained from ATCC. These cells were modified via the CRISPR-Cas9 gene editing system to knockout the *CFTR* gene on both alleles for a homozygous KO. To use as a WT cell line, Caco2 cells were treated with a non-targeting CRISPR-Cas9 gene editing. All experiments were conducted using these *CFTR* KO (D8) and a *CFTR* WT (Y21) cell lines.

MTT Assay

The Y21 and D8 cells were plated at 4,000 cells/well in a 96 well plate and incubated 37°C for 24 hours. The cells were then treated with .1uM Thapsigargin (Catalog # T9033, Sigma-Aldrich) to induce the UPR (Chidawanyika, Sergison, Cole, Mark, & Supattapone, 2018). The cells were treated with the MTT reagent at various time points. MTT dye is reduced by NADPH-reductase enzymes, resulting in production of insoluble, purple-colored formazan (Pascua-Maestro *et al.*, 2018), giving an indication

of cell viability at different points after the treatment. After four hours, a solubilization reagent was added, and the cells were incubated overnight before being read on a plate reader for absorbance at 595nm, and then read for background at 660nm. The MTT dye was added to five different plates at varying timepoints: 2 hours, 24 hours, 48 hours, 72 hours and 96 hours. All time points were normalized to an untreated, 0 hour plate to account for differences in growth between the two different cell lines.

SRB Assay

The cells were plated at 4,000 cells/well in a 96 well plate and incubated at 37°C for 24 hours. The cells were then treated with .1µM Thapsigargin (Catalog # T9033, Sigma-Aldrich) to induce the UPR (Chidawanyika, Sergison, Cole, Mark, & Supattapone, 2018). The cells were then fixed, at various time points, using ice-cold PBS for approximately 10 minutes. The cells were placed in a dry incubator at 37°C for 1 hour to dry completely. At this point, the plate can be left at room temperature indefinitely until the next step. The cells were treated with 50ul of .04% SRB solution in 1% acetic acid and incubated at room temperature for 1 hour. The cells were rinsed 3X with 1% acetic acid to remove excess SRB solution. SRB binds to protein, and provides an indication of cellular protein content, and therefore cell density (Vichai & Kirtikara, 2006). The plates were dried in the dry incubator for 1-2 hours, or until all liquid has evaporated. At this point, the plate can be left at room temperature indefinitely until the next step. The cells were treated with 100ul of 10M Tris and incubated for 5 minutes to resuspend the SRB with their bound proteins. The cells were read on a plate reader at 540nm to measure the absorbance of the SRB signal. Similar to the MTT assay, the SRB

assay was started on five different plates at various times after treatment: 2 hours, 24 hours, 48 hours, 72 hours and 96 hours.

Results

CFTR KO/WT Cells Response to ER Stress through Unfolded Protein Response

To determine the role of CFTR in the unfolded protein response due to ER stress, I ran MTT and SRB assays to measure the viability and protein concentration in *CFTR* WT and KO cell lines after treatment with Thapsigargin, which induces ER stress.

The MTT assay revealed a significant difference between the *CFTR* KO and WT cell lines at several of the time points (Figure 43). The SRB assay revealed a similar trend, although the significant time points were slightly varied from the MTT assay (Figure 43).

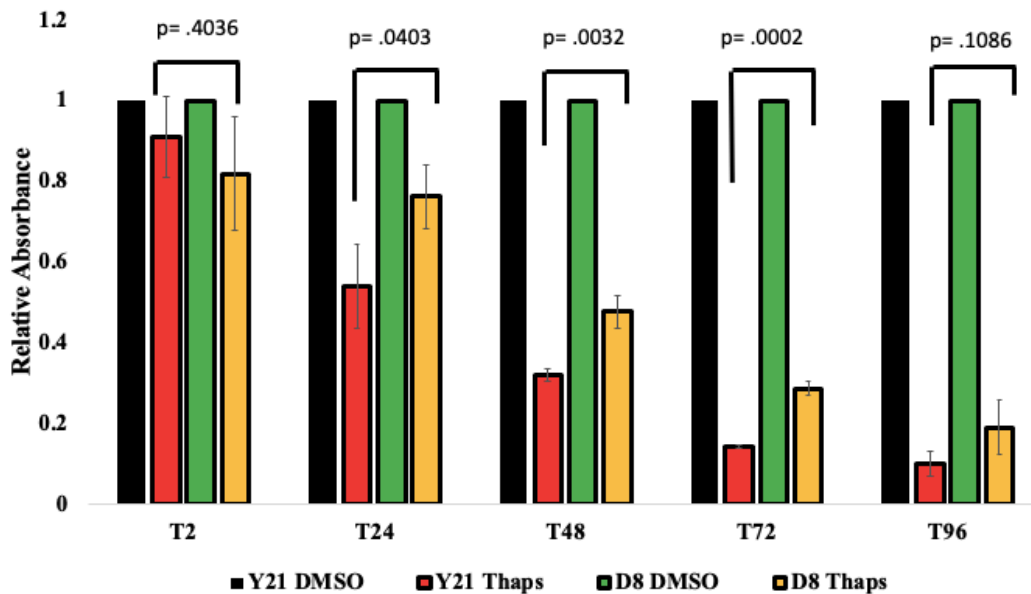


Figure 42: MTT assay, with Y21 (*CFTR* WT) and D8 (*CFTR* KO) Caco2 cell lines, treated with .1 μ M Thapsigargin to induce ER stress. *CFTR* KO cells have a significantly better survival compared to the *CFTR* WT. Three replicates, p values from 2-tailed T-tests

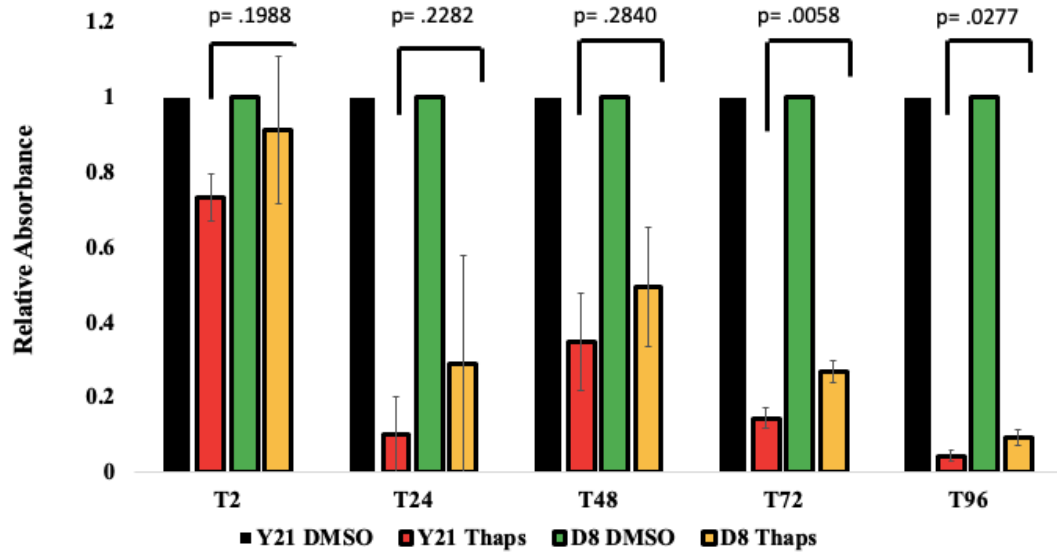


Figure 43: SRB assay, with Y21 (*CFTR* WT) and D8 (*CFTR* KO) Caco2 cell lines, treated with .1uM Thapsigargin to induce ER stress. *CFTR* KO cells have a significantly better survival compared to the *CFTR* WT at several time points. Three replicates, p values from 2-tailed T-tests

Additional

RT-qPCR Primers

18S

Forward: 5' CGCCGCTAGAGGTGAAATTCTT 3'

Reverse: 5' CAGTCGGCATCGTTTATGGTC 3'

150bp

KCNQ1

Forward: 5' GCGGAAGCCTTACGATGTG 3'

Reverse: 5' CCTTGTCTTCTACTCGGTTTCAGG 3'

200bp

KCNQ1OT1

Forward: 5' TGGTCTGGTGGGCTTTTGTT 3'

Reverse: 5' GGGACACAGGAGTGTAAGCC 3'

128bp

β -catenin (CTNNB1)

Forward: 5' TCTGATAAAGGCTACTGTTGGATTGA 3'

Reverse: 5' TCAGCGAAAGGTGCATGATT 3'

CDKN1C

Forward: 5' GTGAGCCAATTTAGAGCCCAA 3'

Reverse: 5' CGGTTGCTGCTACATGAACG 3'

References

1. Abbott, G.W. (2014). Biology of the KCNQ1 potassium channel. *New Journal of Science*, 2014, ID 237431
2. Alzamora, R., O'Mahony, F., Ko, W.-H., Yip, T. W.-N., Carter, D., Irnaten, M., & Harvey, B. J. (2011). Berberine Reduces cAMP-Induced Chloride Secretion in T84 Human Colonic Carcinoma Cells through Inhibition of Basolateral KCNQ1 Channels. *Frontiers in Physiology*, 2. <https://doi.org/10.3389/fphys.2011.00033>
3. American Cancer Society (2018). Colorectal Cancer stages. *ACS Colorectal Cancer*.
4. Anderson, E.C., Hessman, C., Levin, T.G., Monroe, M.M., & Wong, M.H. (2011). Role of colorectal cancer stem cells in metastatic disease and therapeutic response. *Cancers*, 3, 319-339.
5. Asahara, S., Etoh, H., Inoue, H., Teruyama, K., Shibutani, Y., Ihara, Y., Kawada, Y., Bartolome, A., Hashimoto, N., Matsuda, T., Koyanagi-Kimura, M., Kanno, A., Hirota, Y., Hosooka, T., Nagshima, K., Nishimura, W., Inoue, H., Matsumoto, M., Higgins, M.J., Yasuda, K., Inagaki, N., Seino, S., & Kasuga, M., Kido, Y. (2015). Paternal allelic mutation at the *Kcnq1* locus reduces pancreatic β -cell mass by epigenetic modification of *Cdkn1c*. *Proceedings of the National Academy of Sciences*, 112(27), 8332–8337. <https://doi.org/10.1073/pnas.1422104112>
6. Barker, N., van Es, J. H., Kuipers, J., Kujala, P., van den Born, M., Cozijnsen, M., Haegebarth, A., Korving, J., Begthel, H., Peters, P.J., & Clevers, H. (2007). Identification of stem cells in small intestine and colon by marker gene *Lgr5*. *Nature*, 449(7165), 1003–1007. <https://doi.org/10.1038/nature06196>
7. Beumer, J., & Clevers, H. (2016). Regulation and plasticity of intestinal stem cells during homeostasis and regeneration. *Development*, 143(20), 3639–3649. <https://doi.org/10.1242/dev.133132>
8. Bramsen, J. B., Rasmussen, M. H., Ongen, H., Mattesen, T. B., Ørntoft, M.-B. W., Árnadóttir, S. S., Sandoval, J., Laguna, T., Vang, S., Oster, B., Lamy, P., Madsen, M.R., Laurberg, S., Esterller, M., Dermitzakis, E.T., Omtoft, T.F., & Andersen, C. L. (2017). Molecular-Subtype-Specific Biomarkers Improve Prediction of Prognosis in Colorectal Cancer. *Cell Reports*, 19(6), 1268–1280. <https://doi.org/10.1016/j.celrep.2017.04.045>
9. Bustos, V. A., Rapetti-Maus, R., Nolan, A., Lajczak, N. K., Harvey, H., Thomas, W., & Harvey, B. J. (2015). Beta-catenin regulates KCNQ1 potassium channel expression in colon cancer cells. *Proceedings of The Physiological Society, Proc Physiol Soc 34*. Retrieved from <http://www.physoc.org/proceedings/abstract/Proc%20Physiol%20Soc%2034C49>
10. Cabrera, M. C., Hollingsworth, R. E., & Hurt, E. M. (2015). Cancer stem cell plasticity and tumor hierarchy. *World Journal of Stem Cells*, 7(1), 27–36. <https://doi.org/10.4252/wjsc.v7.i1.27>
11. Cammareri, P., Vincent, D. F., Hodder, M. C., Ridgway, R. A., Murgia, C., Nobis, M., Campbell, A.D., Varga, J., Huels, D.J., Subramani, C., Prescott, K.L.H., Nixon, C., Hedley, A., Barry, S.T., Greten, F.R., Inman, G.J., & Sansom, O. J. (2017). TGF β pathway limits dedifferentiation following WNT and MAPK pathway activation to

- suppress intestinal tumorigenesis. *Cell Death and Differentiation*, 24(10), 1681–1693. <https://doi.org/10.1038/cdd.2017.92>
12. Chen, W., Dong, J., Haiech, J., Kilhoffer, M.-C., & Zeniou, M. (2016). Cancer Stem Cell Quiescence and Plasticity as Major Challenges in Cancer Therapy. *Stem Cells International*, 2016. <https://doi.org/10.1155/2016/1740936>
 13. Cheng, S. H., Gregory, R. J., Marshall, J., Paul, S., Souza, D. W., White, G. A., O'Riordan, C.R., & Smith, A. E. (1990). Defective intracellular transport and processing of CFTR is the molecular basis of most cystic fibrosis. *Cell*, 63(4), 827–834. [https://doi.org/10.1016/0092-8674\(90\)90148-8](https://doi.org/10.1016/0092-8674(90)90148-8)
 14. Chidawanyika, T., Sergison, E., Cole, M., Mark, K., & Supattapone, S. (2018). SEC24A identified as an essential mediator of thapsigargin-induced cell death in a genome-wide CRISPR/Cas9 screen. *Cell Death Discovery*, 4(1), 115. <https://doi.org/10.1038/s41420-018-0135-5>
 15. Chiesa, N., De Crescenzo, A., Mishra, K., Perone, L., Carella, M., Palumbo, O., Mussa, A., Sparago, A., Cerrato, F., Russo, S., Lapi, E., Cubellis, M.V., Kanduri, C., Silengo, M.C., Riccio, A., & Ferrero, G. B. (2012). The KCNQ1OT1 imprinting control region and non-coding RNA: new properties derived from the study of Beckwith-Wiedemann syndrome and Silver-Russell syndrome cases. *Human Molecular Genetics*, 21(1), 10–25. <https://doi.org/10.1093/hmg/ddr419>
 16. Clevers, H. (2006). Wnt/ β -Catenin Signaling in Development and Disease. *Cell*, 127(3), 469–480. <https://doi.org/10.1016/j.cell.2006.10.018>
 17. Colorectal Cancer Stages. Retrieved November 21, 2018, from <https://www.cancer.org/cancer/colon-rectal-cancer/detection-diagnosis-staging/staged.html>
 18. Crotti, L., Celano, G., Dagradi, F., & Schwartz, P. J. (2008). Congenital long QT syndrome. *Orphanet Journal of Rare Diseases*, 3, 18. <https://doi.org/10.1186/1750-1172-3-18>
 19. de Lau, W., Barker, N., Low, T. Y., Koo, B.-K., Li, V. S. W., Teunissen, H., Kujala, P., Haegerbarth, A., Peters, P.J., van de Wetering, M., Stange, D.E., van E, J.E., Guardavaccaro, D., Schasfoort, R.B.M., Mohri, Y., Nishimori, K., Mohammed, S., Heck, A.J.R., & Clevers, H. (2011). Lgr5 homologues associate with Wnt receptors and mediate R-spondin signalling. *Nature*, 476(7360), 293–297. <https://doi.org/10.1038/nature10337>
 20. den Uil, S. H., Coupé, V. M. H., Linnekamp, J. F., van den Broek, E., Goos, J. A. C. M., Delis-van Diemen, P. M., Belt, E.J.T., van Grieken, N.C.T., Scott, P.M., Vermeulen, L., Medema, J.P., Bril, H., Stockmann, H.B.A.C., Cormier, R.T., Meijer, G.A., & Fijneman, R. J. A. (2016). Loss of KCNQ1 expression in stage II and stage III colon cancer is a strong prognostic factor for disease recurrence. *British Journal of Cancer*, 115(12), 1565–1574. <https://doi.org/10.1038/bjc.2016.376>
 21. Dow, L. E., O'Rourke, K. P., Simon, J., Tschaharganeh, D. F., van Es, J. H., Clevers, H., & Lowe, S. W. (2015). Apc restoration promotes cellular differentiation and reestablishes crypt homeostasis in colorectal cancer. *Cell*, 161(7), 1539–1552. <https://doi.org/10.1016/j.cell.2015.05.033>
 22. Duong, C. (2014). Generation of novel chimeric antigen receptors to enhance the specificity and activity of T cells for the adoptive immunotherapy for cancer. Retrieved from <http://minerva-access.unimelb.edu.au/handle/11343/44219>

23. Eggermann, T., Eggermann, K., & Schönherr, N. (2008). Growth retardation versus overgrowth: Silver-Russell syndrome is genetically opposite to Beckwith-Wiedemann syndrome. *Trends in Genetics*, *24*(4), 195–204. <https://doi.org/10.1016/j.tig.2008.01.003>
24. Elborn, J. S. (2016). Cystic fibrosis. *The Lancet*, *388*(10059), 2519–2531. [https://doi.org/10.1016/S0140-6736\(16\)00576-6](https://doi.org/10.1016/S0140-6736(16)00576-6)
25. Fakih, M. G. (2015). Metastatic Colorectal Cancer: Current State and Future Directions. *Journal of Clinical Oncology*, *33*(16), 1809–1824. <https://doi.org/10.1200/JCO.2014.59.7633>
26. Fearon, E. R., & Vogelstein, B. (1990). A genetic model for colorectal tumorigenesis. *Cell*, *61*(5), 759–767. [https://doi.org/10.1016/0092-8674\(90\)90186-I](https://doi.org/10.1016/0092-8674(90)90186-I)
27. Fleming, M., Ravula, S., Tatishchev, S. F., & Wang, H. L. (2012). Colorectal carcinoma: Pathologic aspects. *Journal of Gastrointestinal Oncology*, *3*(3), 153–173. <https://doi.org/10.3978/j.issn.2078-6891.2012.030>
28. Flier, L. G. van der, & Clevers, H. (2009). Stem Cells, Self-Renewal, and Differentiation in the Intestinal Epithelium. *Annual Review of Physiology*, *71*(1), 241–260. <https://doi.org/10.1146/annurev.physiol.010908.163145>
29. Gray, J. P., Karandrea, S., Burgos, D. Z., Jaiswal, A. A., & Heart, E. A. (2016). NAD(P)H-dependent Quinone Oxidoreductase 1 (NQO1) and Cytochrome P450 Oxidoreductase (CYP450OR) differentially regulate menadione-mediated alterations in redox status, survival and metabolism in pancreatic β -cells. *Toxicology Letters*, *262*, 1–11. <https://doi.org/10.1016/j.toxlet.2016.08.021>
30. Greaves, M., & Maley, C. C. (2012). Clonal evolution in cancer. *Nature*, *481*(7381), 306–313. <https://doi.org/10.1038/nature10762>
31. Grootjans, J., Kaser, A., Kaufman, R. J., & Blumberg, R. S. (2016). The unfolded protein response in immunity and inflammation. *Nature Reviews Immunology*, *16*(8), 469–484. <https://doi.org/10.1038/nri.2016.62>
32. Haegerbarth, A., & Clevers, H. (2009). Wnt Signaling, Lgr5, and Stem Cells in the Intestine and Skin. *The American Journal of Pathology*, *174*(3), 715–721. <https://doi.org/10.2353/ajpath.2009.080758>
33. He, X. C., Zhang, J., Tong, W.-G., Tawfik, O., Ross, J., Scoville, D. H., Tian, Q., Zeng, X., He, X., Wiedemann, L.M., Mishina, Y., & Li, L. (2004). BMP signaling inhibits intestinal stem cell self-renewal through suppression of Wnt- β -catenin signaling. *Nature Genetics*, *36*(10), 1117–1121. <https://doi.org/10.1038/ng1430>
34. Higashimoto, K., Soejima, H., Saito, T., Okumura, K., & Mukai, T. (2006). Imprinting disruption of the CDKN1C/KCNQ1OT1 domain: the molecular mechanisms causing Beckwith-Wiedemann syndrome and cancer. *Cytogenetic and Genome Research*, *113*(1–4), 306–312. <https://doi.org/10.1159/000090846>
35. H'mida Ben-Brahim, D., Hammami, S., Haddaji Mastouri, M., Trabelsi, S., Chourabi, M., Sassi, S., Mougou, S., Gribaa, M., Zakhama, A., Guediche, M.N., & Saad, A. (2015). Partial KCNQ1OT1 hypomethylation: A disguised familial Beckwith-Wiedemann syndrome as a sporadic adrenocortical tumor. *Applied & Translational Genomics*, *4*, 1–3. <https://doi.org/10.1016/j.atg.2014.10.001>
36. Hong, S. P., Min, B. S., Kim, T. I., Cheon, J. H., Kim, N. K., Kim, H., & Kim, W. H. (2012). The differential impact of microsatellite instability as a marker of prognosis and tumour response between colon cancer and rectal cancer. *European Journal of*

- Cancer*, 48(8), 1235–1243. <https://doi.org/10.1016/j.ejca.2011.10.005>Izsvák, Z., & Ivics, Z. (2004). Sleeping Beauty Transposition: Biology and Applications for Molecular Therapy. *Molecular Therapy*, 9(2), 147–156. <https://doi.org/10.1016/j.ymthe.2003.11.009>
37. Jadhav, U., Saxena, M., O'Neill, N. K., Saadatpour, A., Yuan, G.-C., Herbert, Z., Murata, K., & Shivdasani, R. A. (2017). Dynamic Reorganization of Chromatin Accessibility Signatures during Dedifferentiation of Secretory Precursors into Lgr5+ Intestinal Stem Cells. *Cell Stem Cell*, 21(1), 65-77.e5. <https://doi.org/10.1016/j.stem.2017.05.001>
38. Jones, M. J., Bogutz, A. B., & Lefebvre, L. (2011). An Extended Domain of Kcnq1ot1 Silencing Revealed by an Imprinted Fluorescent Reporter ν . *Molecular and Cellular Biology*, 31(14), 2827–2837. <https://doi.org/10.1128/MCB.01435-10>
39. Kanduri, C. (2016). Long noncoding RNAs: Lessons from genomic imprinting. *Biochimica et Biophysica Acta (BBA) - Gene Regulatory Mechanisms*, 1859(1), 102–111. <https://doi.org/10.1016/j.bbagr.2015.05.006>
40. Kasuga, M. (2011). KCNQ1, a susceptibility gene for type 2 diabetes. *Journal of Diabetes Investigation*, 2(6), 413–414. <https://doi.org/10.1111/j.2040-1124.2011.00178.x>
41. Kather, J. N., Halama, N., & Jaeger, D. (2018). Genomics and emerging biomarkers for immunotherapy of colorectal cancer. *Seminars in Cancer Biology*, 52, 189–197. <https://doi.org/10.1016/j.semcancer.2018.02.010>
42. Katz, L. H., Likhter, M., Jogunoori, W., Belkin, M., Ohshiro, K., & Mishra, L. (2016). TGF- β signaling in liver and gastrointestinal cancers. *Cancer Letters*, 379(2), 166–172. <https://doi.org/10.1016/j.canlet.2016.03.033>
43. Kerem, B. S., Buchanan, J. A., Durie, P., Corey, M. L., Levison, H., Rommens, J. M., Buchwald, M., & Tsui, L. C. (1989). DNA marker haplotype association with pancreatic sufficiency in cystic fibrosis. *American Journal of Human Genetics*, 44(6), 827–834.
44. Kim, K.-A., Wagle, M., Tran, K., Zhan, X., Dixon, M. A., Liu, S., Gros, D., Korver, W., Yonkovich, S., Tomasevic, N., Binnerts, M., & Abo, A. (2008). R-Spondin Family Members Regulate the Wnt Pathway by a Common Mechanism. *Molecular Biology of the Cell*, 19(6), 2588–2596. <https://doi.org/10.1091/mbc.e08-02-0187>
45. Kleme, M.-L., Sané, A. T., Garofalo, C., & Levy, E. (2016). Targeted CFTR gene disruption with zinc-finger nucleases in human intestinal epithelial cells induces oxidative stress and inflammation. *The International Journal of Biochemistry & Cell Biology*, 74, 84–94. <https://doi.org/10.1016/j.biocel.2016.02.022>
46. Kreso, A., & Dick, J. E. (2014). Evolution of the Cancer Stem Cell Model. *Cell Stem Cell*, 14(3), 275–291. <https://doi.org/10.1016/j.stem.2014.02.006>
47. Liu, H., Wu, W., Liu, Y., Zhang, C., & Zhou, Z. (2014). Predictive value of cystic fibrosis transmembrane conductance regulator (CFTR) in the diagnosis of gastric cancer. *Clinical and Investigative Medicine. Medecine Clinique Et Experimentale*, 37(4), E226-232.
48. Liu, K., Zhang, X., Zhang, J. T., Tsang, L. L., Jiang, X., & Chan, H. C. (2016). Defective CFTR- β -catenin interaction promotes NF- κ B nuclear translocation and intestinal inflammation in cystic fibrosis. *Oncotarget*, 7(39), 64030–64042. <https://doi.org/10.18632/oncotarget.11747>

49. Mah, A. T., Yan, K. S., & Kuo, C. J. (2016). Wnt pathway regulation of intestinal stem cells. *The Journal of Physiology*, *594*(17), 4837–4847. <https://doi.org/10.1113/JP271754>
50. Mancini-DiNardo, D., Steele, S. J. S., Levorse, J. M., Ingram, R. S., & Tilghman, S. M. (2006). Elongation of the *Kcnqlot1* transcript is required for genomic imprinting of neighboring genes. *Genes & Development*, *20*(10), 1268–1282. <https://doi.org/10.1101/gad.1416906>
51. Mohammad, F., Mondal, T., Guseva, N., Pandey, G. K., & Kanduri, C. (2010). *Kcnqlot1* noncoding RNA mediates transcriptional gene silencing by interacting with *Dnmt1*. *Development*, *137*(15), 2493–2499. <https://doi.org/10.1242/dev.048181>
52. NIH. (2018). Cancer Stat Facts: Colorectal Cancer. *NIH: Surveillance, Epidemiology, and End Results Program*.
53. Nolan, P. M., Kapfhamer, D., & Bućan, M. (1997). Random Mutagenesis Screen for Dominant Behavioral Mutations in Mice. *Methods*, *13*(4), 379–395. <https://doi.org/10.1006/meth.1997.0545>
54. O'Rourke, K. P., Dow, L. E., & Lowe, S. W. (2016). Immunofluorescent Staining of Mouse Intestinal Stem Cells. *Bio-Protocol*, *6*(4).
55. Pandey, R. R., Mondal, T., Mohammad, F., Enroth, S., Redrup, L., Komorowski, J., Nagano, T., Mancini-DiNardo, D., & Kanduri, C. (2008). *Kcnqlot1* Antisense Noncoding RNA Mediates Lineage-Specific Transcriptional Silencing through Chromatin-Level Regulation. *Molecular Cell*, *32*(2), 232–246. <https://doi.org/10.1016/j.molcel.2008.08.022>
56. Pascua-Maestro, R., Corraliza-Gomez, M., Diez-Hermano, S., Perez-Segurado, C., Ganfornina, M. D., & Sanchez, D. (2018). The MTT-formazan assay: Complementary technical approaches and in vivo validation in *Drosophila* larvae. *Acta Histochemica*, *120*(3), 179–186. <https://doi.org/10.1016/j.acthis.2018.01.006>
57. Rafeeq, M. M., & Murad, H. A. S. (2017). Cystic fibrosis: current therapeutic targets and future approaches. *Journal of Translational Medicine*, *15*. <https://doi.org/10.1186/s12967-017-1193-9>
58. Rao, C. V., & Yamada, H. Y. (2013). Genomic Instability and Colon Carcinogenesis: From the Perspective of Genes. *Frontiers in Oncology*, *3*. <https://doi.org/10.3389/fonc.2013.00130>
59. Rapetti-Mauss, R., Bustos, V., Thomas, W., McBryan, J., Harvey, H., Lajczak, N., Madden, S.F., Pellissier, B., Borgese, F., Soriani, O., & Harvey, B. J. (2017). Bidirectional *KCNQ1*: β -catenin interaction drives colorectal cancer cell differentiation. *Proceedings of the National Academy of Sciences*, 201702913. <https://doi.org/10.1073/pnas.1702913114>
60. CFTR gene. Retrieved February 1, 2019, from Genetics Home Reference website: <https://ghr.nlm.nih.gov/gene/CFTR>
61. Reya, T., & Clevers, H. (2005). Wnt signalling in stem cells and cancer. *Nature*, *434*(7035), 843–850. <https://doi.org/10.1038/nature03319>
62. Riihimäki, M., Hemminki, A., Sundquist, J., & Hemminki, K. (2016). Patterns of metastasis in colon and rectal cancer. *Scientific Reports*, *6*, 29765. <https://doi.org/10.1038/srep29765>

63. Sancho, R., Cremona, C. A., & Behrens, A. (2015). Stem cell and progenitor fate in the mammalian intestine: Notch and lateral inhibition in homeostasis and disease. *EMBO Reports*, *16*(5), 571–581. <https://doi.org/10.15252/embr.201540188>
64. Schultz, B. M., Gallicio, G. A., Cesaroni, M., Lupey, L. N., & Engel, N. (2015). Enhancers compete with a long non-coding RNA for regulation of the *Kcnq1* domain. *Nucleic Acids Research*, *43*(2), 745–759. <https://doi.org/10.1093/nar/gku1324>
65. Scott, A., Song, J., Ewing, R., & Wang, Z. (2014). Regulation of protein stability of DNA methyltransferase 1 by post-translational modifications. *Acta Biochimica Et Biophysica Sinica*, *46*(3), 199–203. <https://doi.org/10.1093/abbs/gmt146>
66. Seneviratne, D.S. (2014). Hepatocyte Growth Factor Gene Mutation in Human Colorectal Cancer: Causes and Consequences. *PhD Diss., University of Pittsburgh, 2014*
67. Siegel, R. L., Miller, K. D., Fedewa, S. A., Ahnen, D. J., Meester, R. G. S., Barzi, A., & Jemal, A. (2017). Colorectal cancer statistics, 2017. *CA: A Cancer Journal for Clinicians*, *67*(3), 177–193. <https://doi.org/10.3322/caac.21395>
68. Starr, T. K., Allaei, R., Silverstein, K. A. T., Staggs, R. A., Sarver, A. L., Bergemann, T. L., Gupta, M., O'Sullivan, G., Matise, I., Dupuy, A.J., Collier, L.S., Powers, S., Oberg, A.L., Asmann, Y.W., Thibodeau, S.N., Tessarollo, L., Copeland, N.G., Jenkins, N.A., Cormier, R.T., & Largaespada, D. A. (2009). A Transposon-Based Genetic Screen in Mice Identifies Genes Altered in Colorectal Cancer. *Science (New York, N.Y.)*, *323*(5922), 1747–1750. <https://doi.org/10.1126/science.1163040>
69. Strubberg, A. M., Liu, J., Walker, N. M., Stefanski, C. D., MacLeod, R. J., Magness, S. T., & Clarke, L. L. (2018). Cfr Modulates Wnt/ β -Catenin Signaling and Stem Cell Proliferation in Murine Intestine. *Cellular and Molecular Gastroenterology and Hepatology*, *5*(3), 253–271. <https://doi.org/10.1016/j.jcmgh.2017.11.013>
70. Strutz-Seebohm, N., Henrion, U., Steinke, K., Tapken, D., Lang, F., & Seebohm, G. (2009). Serum- and Glucocorticoid-inducible Kinases (SGK) regulate KCNQ1/KCNE potassium channels. *Channels*, *3*(2), 88–90. <https://doi.org/10.4161/chan.3.2.8086>
71. Sunamura, N., Ohira, T., Kataoka, M., Inaoka, D., Tanabe, H., Nakayama, Y., Oshimura, M., & Kugoh, H. (2016). Regulation of functional KCNQ1OT1 lncRNA by β -catenin. *Scientific Reports*, *6*, 20690. <https://doi.org/10.1038/srep20690>
72. Tagliaferro, L., Bonawitz, K., Glenn, O. C., & Chiba-Falek, O. (2016). Gene Expression Analysis of Neurons and Astrocytes Isolated by Laser Capture Microdissection from Frozen Human Brain Tissues. *Frontiers in Molecular Neuroscience*, *9*. <https://doi.org/10.3389/fnmol.2016.00072>
73. Taieb, J., Le Malicot, K., Shi, Q., Penault-Llorca, F., Bouché, O., Tabernero, J., Mini, E., Goldberg, R.M., Folprecht, G., Laethem, J.L.V., Sargent, D.J., Alberts, S.R., Emile, J.F., Puig, P.L., & Sinicrope, F. A. (2017). Prognostic Value of BRAF and KRAS Mutations in MSI and MSS Stage III Colon Cancer. *JNCI: Journal of the National Cancer Institute*, *109*(5). <https://doi.org/10.1093/jnci/djw272>
74. Than, B. L. N., Goos, J. A. C. M., Sarver, A. L., O'Sullivan, M. G., Rod, A., Starr, T. K., Fijneman, R.J.A., Meijer, G.A., Zhao, L., Zhang, Y., Largaespada, D.A., Scott, P.M., & Cormier, R. T. (2014). The role of KCNQ1 in mouse and human gastrointestinal cancers. *Oncogene*, *33*(29), 3861–3868. <https://doi.org/10.1038/onc.2013.350>

75. Than, B. L. N., Linnekamp, J. F., Starr, T. K., Largaespada, D. A., Rod, A., Zhang, Y., Bruner, V., Abrahante, J., Schumann, A., Luczak, T., Niemczyk, A., O'Sullivan, M.G., Medema, J.P., Fijneman, R.J.A., Meijer, G.A., den Broek, E.V., Hodges, C.A., Scott, P.M., Vermeulen, L., & Cormier, R. T. (2016). CFTR is a tumor suppressor gene in murine and human intestinal cancer. *Oncogene*, *35*(32), 4179–4187. <https://doi.org/10.1038/onc.2015.483>
76. Umar, S. (2010). Intestinal Stem Cells. *Current Gastroenterology Reports*, *12*(5), 340–348. <https://doi.org/10.1007/s11894-010-0130-3>
77. Valente, F. M., Sparago, A., Freschi, A., Hill-Harfe, K., Maas, S. M., Frints, S. G. M., Alders, M., Pignata, L., Franzese, M., Angelini, C., Carli, D., Mussa, A., Gazzin, A., Gabbarini, F., Acurzio, B., Ferrero, G.B., Blik, J., Williams, C.A., Riccio, A., & Cerrato, F. (2019). Transcription alterations of KCNQ1 associated with imprinted methylation defects in the Beckwith-Wiedemann locus. *Genetics in Medicine: Official Journal of the American College of Medical Genetics*. <https://doi.org/10.1038/s41436-018-0416-7>
78. Valkenburg, K. C., Graveel, C. R., Zylstra-Diegel, C. R., Zhong, Z., & Williams, B. O. (2011). Wnt/ β -catenin Signaling in Normal and Cancer Stem Cells. *Cancers*, *3*(2), 2050–2079. <https://doi.org/10.3390/cancers3022050>
79. Vichai, V., & Kirtikara, K. (2006). Sulforhodamine B colorimetric assay for cytotoxicity screening. *Nature Protocols*, *1*(3), 1112–1116. <https://doi.org/10.1038/nprot.2006.179>
80. Villa, C., & Combi, R. (2016). Potassium Channels and Human Epileptic Phenotypes: An Updated Overview. *Frontiers in Cellular Neuroscience*, *10*. <https://doi.org/10.3389/fncel.2016.00081>
81. Vyas, B., Puri, R. D., Namboodiri, N., Nair, M., Sharma, D., Movva, S., Saxena, R., Bohora, S., Aggarwal, N., Vora, A., Kumar, J., Singh, T., & Verma, I. C. (2016). KCNQ1 mutations associated with Jervell and Lange-Nielsen syndrome and autosomal recessive Romano-Ward syndrome in India-expanding the spectrum of long QT syndrome type 1. *American Journal of Medical Genetics. Part A*, *170*(6), 1510–1519. <https://doi.org/10.1002/ajmg.a.37636>
82. Warth, R., Garcia Alzamora, M., Kim, J., Zdebik, A., Nitschke, R., Bleich, M., Gerlach, U., Barhanin, J., & Kim, S. (2002). The role of KCNQ1/KCNE1 K⁺ channels in intestine and pancreas: lessons from the KCNE1 knockout mouse. *Pflügers Archiv*, *443*(5), 822–828. <https://doi.org/10.1007/s00424-001-0751-3>
83. Weksberg, R., Shuman, C., Caluseriu, O., Smith, A.C., Fei, Y.L., Nishikawa, J., Stockley, T.L., Best, L., Chitayat, D., Olney, A., Ives, E., Schneider, A., Bestor T.H., Li, M., Sadowski, P., Squire, J. (2002). Discordant KCNQ1OT1 imprinting in sets of monozygotic twins discordant for Beckwith-Wiedemann syndrome. *Human Molecular Genetics*, *15* (11): 1317-1325
84. Weksberg, R., Smith, A. C., Squire, J., & Sadowski, P. (2003). Beckwith–Wiedemann syndrome demonstrates a role for epigenetic control of normal development. *Human Molecular Genetics*, *12*(suppl_1), R61–R68. <https://doi.org/10.1093/hmg/ddg067>
85. World Cancer Research Fund. (2018). Colorectal cancer statistics. *Continuous Update Project*.

86. Xiao, Y., & Freeman, G. J. (2015). The Microsatellite Instable (MSI) Subset of Colorectal Cancer is a particularly good candidate for checkpoint blockade immunotherapy. *Cancer Discovery*, 5(1), 16–18. <https://doi.org/10.1158/2159-8290.CD-14-1397>
87. Zhang, J., Wang, Y., Jiang, X., & Chan, H. C. (2018). Cystic fibrosis transmembrane conductance regulator-emerging regulator of cancer. *Cellular and Molecular Life Sciences: CMLS*, 75(10), 1737–1756. <https://doi.org/10.1007/s00018-018-2755-6>
88. <https://www.cff.org/Life-With-CF/Transitions/Colorectal-Cancer-and-CF/About-Colorectal-Cancer/>
89. <http://switchgeargenomics.com/lightswitch-luciferase-assay-system-reagent-kit>